

Linked Cluster Expansion Around Mean-Field Theories of Interacting Electrons

V. Janiš

*Institute of Physics, Academy of Sciences of the Czech Republic,
CZ-18040 Praha 8, Czech Republic*

J. Schlipf

*Institut für Theoretische Physik C, Technische Hochschule Aachen,
D-52056 Aachen, Federal Republic of Germany*

A general expansion scheme based on the concept of linked cluster expansion from the theory of classical spin systems is constructed for models of interacting electrons. It is shown that with a suitable variational formulation of mean-field theories at weak (Hartree-Fock) and strong (Hubbard-III) coupling the expansion represents a universal and comprehensive tool for systematic improvements of static mean-field theories. As an example of the general formalism we investigate in detail an analytically tractable series of ring diagrams that correctly capture dynamical fluctuations at weak coupling. We introduce renormalizations of the diagrammatic expansion at various levels and show how the resultant theories are related to other approximations of similar origin. We demonstrate that only fully self-consistent approximations produce global and thermodynamically consistent extensions of static mean field theories. A fully self-consistent theory for the ring diagrams is reached by summing the so-called noncrossing diagrams.

Preprint-no. RWTH-ITP-C 5/95

I. INTRODUCTION

A first step towards a global description of a model that cannot be solved exactly is a mean-field theory (MFT). It usually shares many features with an exact solution, offers a global phase diagram, and enables to investigate the existence of various solutions that exhibit long-range order. A comprehensive MFT represents a conserving and thermodynamically consistent approximation, i.e. there exists an explicit free energy functional applicable in the entire range of input parameters.

In the theory of interacting electrons it was for a long time only the weak-coupling Hartree-Fock solution that fulfilled the usual requirements imposed on a MFT in classical statistical mechanics of lattice spin systems [1]. Attempts to construct a strong-coupling MFT around the atomic limit with analogous comprehensive properties failed in most cases to produce a thermodynamically consistent MFT. In the case of the Hubbard model mean-field theories reproducing the atomic limit have a structure of the Hubbard-III solution [2] and are commonly called alloy-analogy approximations [3,4]. These approximations suffer from the deficiency that they do not represent a conserving approximation in the sense of Baym [5]. Only lately in connection with the limit of high spatial dimensions, $d \rightarrow \infty$, a thermodynamically consistent extension of the Hubbard-III solution with a free-energy functional was proposed [6].

However, having a thermodynamically consistent MFT alone is insufficient to make the mean-field results reliable. Unless we have an expansion scheme around the MFT with which we can study the stability of the mean-field solution, we cannot really judge whether and in which limit the mean field produces physically relevant results. Hence it is part of the construction of a comprehensive MFT to find an appropriate perturbation theory the first term of which is just the mean-field grand potential. It is fairly known that the Hartree-Fock MFT is a first, self-consistent approximation of the weak-coupling perturbation expansion. It is, however, much more difficult to find an expansion scheme the first step of which would be a MFT of the Hubbard-III type, since this MFT cannot be mapped onto a Fermi gas. We cannot use a usual expansion relying on Gaussian integration and the Wick theorem.

We are hence facing the problem how to connect a general MFT with an appropriate perturbation theory. First attempts to abandon the weak-coupling expansion in the Hubbard model were made by Hubbard [7] who formulated an unrenormalized expansion in the hopping amplitude within which he rederived an approximation now called Hubbard-I. Recently Metzner [8] using a formulation in $d = \infty$ extended the Hubbard approach and showed a way how renormalizations from the linked cluster expansion [9] can be introduced. However, it has proved cumbersome to deal with renormalizations effectively because of the quantum character of the model. This expansion does not efficiently go beyond the Hubbard-III solution and in this form it seems inadequate to improve strong-coupling mean-field theories.

It is the aim of this paper to formulate an expansion scheme suitable to encompass general mean-field theories, the Hartree-Fock at weak coupling as well as the Hubbard-III at strong coupling, which enables to introduce consistently renormalizations leading to conserving approximations in the Baym sense. Importance of a systematic expansion

around a comprehensive MFT was recently acknowledged in [1], where a formal perturbation expansion resulted from a specific variational formulation of mean-field theories being either an upper bound (Hartree-Fock) or a lower bound (extension of Hubbard-III from [6]). In the following we formulate this expansion explicitly, show how to generate various approximations, how to introduce renormalizations, and study quantitatively the effects of dynamical fluctuations on the results of static mean-field theories. We use the linked cluster expansion (LCE) from the classical statistical theory of liquids and lattice spin systems reviewed in [9]. The LCE is applied here in quite a different manner than in [8], since we cannot expand in the hopping amplitude. We formulate the mean-field theories in such a way that we gain a universal expansion scheme for the weak- and strong-coupling theories. Within the derived scheme we compare different approximations having closed form. We further discuss the role and importance of self-consistencies in the light of the recent claim that a partial self-consistency, called iterated perturbation theory, may be superior to the fully self-consistent approach at intermediate and strong coupling [10]. We conclude that only fully self-consistent theories represent conserving approximations. As the main result we then derive a fully self-consistent version of the ring-diagram approximation by summing the so-called “noncrossing” diagrams for the grand potential and thereby win a global, thermodynamically consistent theory containing dynamical fluctuations that is equally applicable to weak as well to strong coupling MFT’s. In this way we remove the doubts that renormalized RPA or more advanced self-consistent approximations may not lead to conserving approximations [11,12].

The paper is organized as follows. In Sec. II we reformulate the variational approach to the construction of the comprehensive MFT from [1] so that the same expansion scheme can be used for the sample mean-field theories of interacting electrons: Hartree-Fock and the thermodynamically consistent extension of Hubbard-III from [6]. Sec. III summarizes the formalism of the LCE needed to generate the appropriate expansion for the grand potential of itinerant models with local electron-electron interaction. In Sec. IV we choose a special class of diagrams, ring diagrams, leading to an approximation in closed form and being exact up to second order in the interaction strength. In Secs. V and VI we derive one-particle properties from the variational grand potential and present numerical results obtained from various simplifications of the ring-diagram approximation. Here the position of the iterated perturbation theory from [10] in the present scheme is thoroughly discussed. In Sec. VII a controlled way to reach full self-consistency and thereby a thermodynamically consistent and conserving theory of the ring-diagram approximation is presented.

II. VARIATIONAL FORMULATION OF MEAN-FIELD THEORIES

A MFT is controllable only if it enables a systematic expansion towards the full solution. Not all constructions of mean-field like approximations are suitable for further corrections via perturbation expansions. E.g. heuristic derivations of the Gutzwiller extension of the Hartree-Fock MFT [13] or of a strong-coupling MFT [2] do not seem to fit into a systematic expansion scheme starting with the MFT. On the other hand, a variational formulation of mean-field theories from [1] offers a consistent way to connect a MFT with a perturbation expansion. We present in this section an analogous variational formulation of mean-field theories of itinerant electrons that enables to formulate a universal expansion scheme for both weak and strong coupling. Explicitly we will refer to the weak-coupling (Hartree-Fock) and strong-coupling (Ref. [1]) theories of the Hubbard model.

For an expansion around a MFT we must decompose the total Hamiltonian into its unperturbed part (leading to the desired MFT) and a perturbation

$$H = H_0 + \Delta H. \quad (1)$$

Our aim is to find suitable constituents of the decomposition (1) for the weak and strong coupling mean-field theories leading to conceptually the same perturbation expansion.

We start with the simpler case of the Hartree-Fock approximation. For the sake of simplicity we restrict ourselves to spatially homogeneous solutions only. The variational parameters in the Hartree-Fock theory are the particle densities n_σ and we can write

$$H = H_{HF} + \Delta H_{HF} \quad (2a)$$

with

$$H_{HF} = -\mathcal{N}U n_\uparrow n_\downarrow + \sum_{\mathbf{k}, \sigma} (\epsilon_{\mathbf{k}} + U n_{-\sigma}) a_{\mathbf{k}\sigma}^\dagger a_{\mathbf{k}\sigma}, \quad (2b)$$

$$\Delta H_{HF} = U \sum_i (\hat{n}_{i\uparrow} - n_\uparrow) (\hat{n}_{i\downarrow} - n_\downarrow), \quad (2c)$$

where $\hat{n}_{i\sigma} = c_{i\sigma}^\dagger c_{i\sigma}$ and \mathcal{N} is the number of lattice sites. This decomposition leads to the standard perturbation expansion around the Hartree-Fock solution generated by the Hamiltonian H_{HF} .

The situation in the case of the strong-coupling MFT is more complicated. The decomposition used in [1] leading to a lower bound does not have the structure of (1). To obtain a structure similar to (2) we have to distinguish the static and dynamic degrees of freedom used in the strong-coupling MFT. We decorate the static degrees of freedom with an index s . We choose a decomposition of the Hubbard Hamiltonian into two Falicov-Kimball subhamiltonians with equal weight $\lambda = 1/2$ [1]. We hence define

$$H_\sigma = \sum_{\mathbf{k}} (\epsilon_{\mathbf{k}} + E_\sigma) a_{\mathbf{k}\sigma}^\dagger a_{\mathbf{k}\sigma} - E_{-\sigma} \sum_i \hat{n}_{i-\sigma}^s + \frac{U}{2} \sum_i \hat{n}_{i\sigma} \hat{n}_{i-\sigma}^s, \quad (3a)$$

where $\hat{n}_{i\sigma}^s = c_{i\sigma}^{s\dagger} c_{i\sigma}^s$ and

$$\Delta H = \sum_{i,\sigma} E_\sigma (\hat{n}_{i\sigma}^s - \hat{n}_{i\sigma}) + \frac{U}{2} \sum_{i,\sigma} \hat{n}_{i\sigma} (\hat{n}_{i-\sigma} - \hat{n}_{i-\sigma}^s) \quad (3b)$$

from which the desired decomposition of the Hubbard Hamiltonian directly follows:

$$H = \sum_{\sigma} H_\sigma + \Delta H. \quad (3c)$$

It is easy to show that $F = -\beta^{-1} \ln \text{Tr} \exp\{-\beta \sum_{\sigma} H_\sigma\}$ in $d = \infty$ generates the mean-field theory of [1] with $\lambda_{at} = 0, \lambda_\sigma = 1/2$. The variational parameters here are not $\hat{n}_{i\sigma}^s$ (which are operators), but energies E_σ . It is also clear from (3a) that the dynamics of H_\uparrow and H_\downarrow decouple and $F_{MF} = F_\uparrow + F_\downarrow$. The stationarity conditions for such a MFT lead to

$$\langle \hat{n}_{i\sigma} \rangle_{MF} = \langle \hat{n}_{i\sigma}^s \rangle_{MF}. \quad (4)$$

We have two different contributions to the perturbation ΔH in (3b), one quadratic and one quartic in creation and annihilation operators. This makes perturbation expansion cumbersome. We can, however, drop the quadratic term without changing the physics of the full Hubbard Hamiltonian. The quadratic term only shifts the spin-dependent chemical potential $\mu_\sigma = \mu + \sigma h$ of the mobile (dynamic) electrons with the energy E_σ playing the role of the chemical potential for the local (static) electrons. These auxiliary local electrons completely decouple from the physical, itinerant electrons in the full solution. The energies E_σ in the physical sector then redefine the origins for the chemical potential μ and the magnetic field h . The physical results do not differ from those obtained from the original Hubbard Hamiltonian without energies E_σ . We can hence choose

$$H = H_{MF} + \Delta H_{MF} = \sum_{\sigma} H_\sigma + \Delta H_{MF} \quad (5a)$$

and

$$\Delta H_{MF} = \frac{U}{2} \sum_{i,\sigma} \hat{n}_{i\sigma} (\hat{n}_{i-\sigma} - \hat{n}_{i-\sigma}^s). \quad (5b)$$

It is worth noting that the decomposition (3)-(5) enabling a systematic perturbation expansion is not derivable for the MFT with $\lambda_\sigma = 1$ and $\lambda_{at} = -1$ as used in [6,14]. To apply decomposition (1) consistently, no negative terms are allowed. If we choose $\lambda_{at} = 0$, the resultant MFT does not reproduce the atomic limit exactly. Although the atomic limit is not covered by (5), due to the halving of the interaction strength in the subhamiltonians \hat{H}_σ , (5) still contains the split-band limit. Important features of (5) are that the mean-field free energy is an exact lower bound to the free energy of the Hubbard model and we can expand consistently around the MFT. Moreover, it was shown earlier in [1] that the choice $\lambda_\sigma = 1$ and $\lambda_{at} = -1$ is equivalent at $T = 0$ to $\lambda_\sigma = 1/2, \lambda_{at} = 0$ with doubled interaction strength U .

Both the mean-field theories for weak and strong coupling now have formally identical structure and the corresponding perturbation expansion can be formulated in the same manner. We use the LCE well elaborated in the classical statistical mechanics [9] as an appropriate tool for our purposes.

III. GENERAL FORMALISM OF THE LINKED CLUSTER EXPANSION

The aim of the LCE is to represent the free energy (grand potential) as an appropriate series generated by derivatives w.r.t. auxiliary external sources added to the unperturbed Hamiltonian. Contrary to the standard weak-coupling expansion, LCE does not rely on the Wick theorem and is hence appropriate for the construction of a systematic expansion around any MFT. The only restriction on applicability of the LCE is that the generating unperturbed functional (free energy of the unperturbed system with suitable external fields) has to be explicitly known.

Our aim is to formulate a perturbation expansion around quantum mean-field theories using decompositions (2) and (3). Although the unperturbed mean-field functional to (2) is known in any dimension, we restrict the expansion to infinite dimensions, since only there the unperturbed functional to the decomposition (3) can explicitly be constructed. This restriction leads to a substantial simplification of the perturbation expansion, since the effective electron propagator in perturbation theory does not depend on momentum explicitly [15].

The generating functional for a quantum LCE can be represented as

$$g_{MF}^{(0)}\{\mu_\sigma, E_\sigma\} = \frac{1}{\mathcal{N}} \ln \text{Tr} \mathcal{T} \exp \left\{ - \int_0^\beta d\tau \left[H_{MF}(\tau) - \sum_{i,\sigma} \mu_\sigma(\tau) \hat{n}_{i\sigma}(\tau) \right] \right\} \quad (6)$$

with \mathcal{T} standing for the time ordering operator and Tr denoting the trace in Fock space. Functional (6) is related to the grand potential $\Omega_{MF}^{(0)} = -\beta^{-1} g_{MF}^{(0)}$. The generating external sources were absorbed into the mean-field variational parameters, n_σ for the weak coupling MFT and E_σ and the chemical potential of the itinerant electrons μ_σ for the strong-coupling MFT. These parameters now become time dependent. They are coupled to the time-dependent particle densities which are the only operators appearing in the perturbation ΔH .

The Hamiltonian in (6) can explicitly be written for the weak-coupling MFT as

$$H_{HF}(\tau) = \sum_{\mathbf{k},\sigma} \epsilon_{\mathbf{k}} a_{\mathbf{k}\sigma}^\dagger(\tau) a_{\mathbf{k}\sigma}(\tau) + U \sum_{i,\sigma} n_{-\sigma}(\tau) (\hat{n}_{i\sigma}(\tau) - n_\sigma) + UN n_\uparrow n_\downarrow, \quad (7a)$$

and for the strong-coupling MFT as

$$H_{MF}(\tau) = \sum_{\mathbf{k},\sigma} \epsilon_{\mathbf{k}} a_{\mathbf{k}\sigma}^\dagger(\tau) a_{\mathbf{k}\sigma}(\tau) + \sum_{i,\sigma} E_\sigma(\tau) (\hat{n}_{i\sigma}(\tau) - \hat{n}_{i\sigma}^s(\tau)) + \frac{U}{2} \sum_{i,\sigma} \hat{n}_{i\sigma}(\tau) \hat{n}_{i-\sigma}^s(\tau). \quad (7b)$$

The time dependency was added to the variational parameters only where necessary. In the limit $d = \infty$ we obtain for the Hartree-Fock MFT

$$g_{HF}^{(0)}\{n_\sigma\} = \int_0^\beta d\tau \left\{ U n_\uparrow n_\downarrow + \sum_\sigma \int_{-\infty}^\infty d\epsilon \rho(\epsilon) [\ln(\partial/\partial\tau + \mu_\sigma - U n_{-\sigma} - \epsilon)](\tau, \tau^+) \right\}, \quad (8a)$$

while for the strong-coupling MFT the generating functional reads

$$\begin{aligned} g_{MF}^{(0)}\{\mu_\sigma, E_\sigma\} = & \sum_\sigma \int_0^\beta d\tau \left\{ \int_{-\infty}^\infty d\epsilon \rho(\epsilon) [\ln(\partial/\partial\tau + \mu_\sigma - E_\sigma - \Sigma_\sigma - \epsilon)](\tau, \tau^+) \right. \\ & + [\ln G_\sigma](\tau, \tau^+) + E_\sigma(\tau) n_\sigma^s(\tau) + (1 - n_{-\sigma}^s(\tau)) ([\ln(\gamma_\sigma)](\tau, \tau^+) - \beta^{-1} \ln(1 - n_{-\sigma}^s(\tau))) \\ & \left. + n_{-\sigma}^s(\tau) \left(\left[\ln \left(\gamma_\sigma - \frac{U}{2} \right) \right](\tau, \tau^+) - \beta^{-1} \ln n_{-\sigma}^s(\tau) \right) \right\}, \quad (8b) \end{aligned}$$

where $n_\sigma(\tau, \tau') := \delta(\tau - \tau') n_\sigma(\tau)$, $E_\sigma(\tau, \tau') := \delta(\tau - \tau') E_\sigma(\tau)$, $\mu_\sigma(\tau, \tau') := \delta(\tau - \tau') \mu_\sigma(\tau)$ and $\gamma_\sigma(\tau, \tau') := G_\sigma^{-1}(\tau, \tau') + \Sigma_\sigma(\tau, \tau')$. The single-particle Green function $G_\sigma(\tau, \tau') = -\langle \mathcal{T} c_\sigma(\tau) c_\sigma^\dagger(\tau') \rangle_T$ and the corresponding self-energy $\Sigma_\sigma(\tau, \tau')$ were used. With these expressions we can derive the explicit LCE with the perturbation $\Delta H(\tau)$ if we use

$$\Delta H_{HF}(\tau) = \frac{1}{U} \frac{\delta}{\delta n_\downarrow(\tau)} \frac{\delta}{\delta n_\uparrow(\tau)}, \quad (9a)$$

$$\Delta H_{MF}(\tau) = -\frac{U}{2} \sum_{\sigma} \frac{\delta}{\delta \mu_{\sigma}(\tau)} \frac{\delta}{\delta E_{-\sigma}(\tau)} \quad (9b)$$

and represent the full potential in $d = \infty$ for the Hartree-Fock MFT as

$$g_{HF} = \ln \left[\exp \left\{ -\frac{1}{U} \int_0^{\beta} d\tau \frac{\delta}{\delta n_{\downarrow}(\tau)} \frac{\delta}{\delta n_{\uparrow}(\tau)} \right\} \exp g_{HF}^{(0)} \{n_{\sigma}\} \right] \quad (10a)$$

and for the strong-coupling MFT as

$$g_{MF} = \ln \left[\exp \left\{ \frac{U}{2} \sum_{\sigma} \int_0^{\beta} d\tau \frac{\delta}{\delta \mu_{\sigma}(\tau)} \frac{\delta}{\delta E_{-\sigma}(\tau)} \right\} \exp g_{MF}^{(0)} \{\mu_{\sigma}, E_{\sigma}\} \right]. \quad (10b)$$

Note that the imaginary time is removed from the variational variables in the end of all calculations to restore the time homogeneity.

The aim of the LCE is to define a direct expansion for the grand potential, i.e. to interchange the logarithm with the variational derivatives in formulas (10). Since the derivatives are of second order, this is a tremendous task and leads to sophisticated rules for the construction of exact contributions in all orders of the perturbation ΔH [9]. We can, however, formally write down the full potential as

$$g_{MF} = \exp \left\{ \frac{U}{2} \sum_{\sigma} \int_0^{\beta} d\tau \left[\frac{\delta}{\delta \mu_{\sigma}(\tau)} \frac{\delta}{\delta E_{-\sigma}(\tau)} \right] \right\} g_{MF}^{(0)} \{\mu_{\sigma}, E_{\sigma}\}. \quad (11)$$

In (11) the brackets with variational derivatives denote a linear operator which commutes with the derivatives and acts on the unperturbed functional $g_{MF}^{(0)}$ as

$$\left[\frac{\delta}{\delta \mu_{\sigma}(\tau)} \frac{\delta}{\delta E_{-\sigma}(\tau)} \right] g_{MF}^{(0)} \{\mu_{\sigma}, E_{\sigma}\} := \frac{\delta^2 g_{MF}^{(0)} \{\mu_{\sigma}, E_{\sigma}\}}{\delta \mu_{\sigma}(\tau) \delta E_{-\sigma}(\tau)} + \frac{\delta g_{MF}^{(0)} \{\mu_{\sigma}, E_{\sigma}\}}{\delta \mu_{\sigma}(\tau)} \frac{\delta g_{MF}^{(0)} \{\mu_{\sigma}, E_{\sigma}\}}{\delta E_{-\sigma}(\tau)}. \quad (12)$$

Definition (12) expresses a derivative w.r.t. a bond (nonlocal) variable (left-hand side) in terms of site (local) variables genuine to the unperturbed functional $g_{MF}^{(0)}$ (right-hand side). The power expansion of the exponential in (11) together with the definition of the bracketed derivative (12) determines the unrenormalized LCE. To save the space we make explicit derivations for the strong-coupling MFT only. We hence drop the subscript ‘‘MF’’ in the forthcoming formulas.

It is convenient as in other perturbation expansions to define a graphical representation for the LCE and to deal with diagrams by introducing vertices and internal lines. If we denote $x_{\sigma}^{\alpha}(\tau)$, $\alpha = \pm$ with $x_{\sigma}^{+}(\tau) = \mu_{\sigma}(\tau) - \mu_{\sigma}$ and $x_{\sigma}^{-}(\tau) = E_{\sigma} - E_{\sigma}(\tau)$ we can define an unrenormalized n -vertex function

$$\Gamma_{(0)}^{(n) \alpha_1 \dots \alpha_n}(\tau_1, \dots, \tau_n) := \frac{\delta^n g^{(0)} \{\mu_{\sigma}, E_{\sigma}\}}{\delta x_{\sigma_1}^{\alpha_1}(\tau_1) \dots \delta x_{\sigma_n}^{\alpha_n}(\tau_n)} \quad (13)$$

and an unrenormalized internal line (edge) $v_{\sigma_1 \sigma_2}^{\alpha_1 \alpha_2}(\tau_1, \tau_2)$ connecting the vertices. The ‘‘propagator’’ is hence a matrix in the internal degrees of freedom of the vertices, α , σ and τ . We can assign a graphical representation to both the vertices and the edges. We denote an n -vertex as



where $1 = (\alpha_1, \sigma_1, \tau_1)$, \dots . In this version of the LCE the electron-electron interaction plays the role of edges connecting the vertices. We assign a dashed line to an edge, i.e.

$$\begin{array}{c} \circ \text{---} \text{---} \text{---} \text{---} \circ \\ 1 \qquad \qquad \qquad 2 \end{array} \longleftrightarrow v_{\sigma_1 \sigma_2}^{\alpha_1 \alpha_2}(\tau_1, \tau_2) := \frac{U}{2} \delta(\tau_1 - \tau_2) \delta_{\sigma_1, -\sigma_2} \delta_{\alpha_1, -\alpha_2}. \quad (14b)$$

With this graphical representation we can try to sum various subclasses of diagrams either with or without renormalizations [9]. The renormalized quantities are standardly denoted with full circles and bold lines, respectively. Note that in the present formulation of the LCE the vertices contain the one-electron propagators (Green functions) while the edges represent the electron-electron correlation.

To obtain a consistent LCE we must treat all the variational functions and parameters that do not serve as generating sources in the unperturbed, mean-field functional as external variables independent of the generating fields. The mean-field stationarity equations, leading to an approximate grand potential of the problem, are imposed only in the end of the calculations after a chosen class of diagrams has been summed up and the time-dependence from the generating fields removed. It is hence necessary to have an expression for the grand potential to be able to expand consistently around a MFT.

IV. RING DIAGRAMS

The LCE is of practical use only if we are able to pick up a class of diagrams that can explicitly be summed and then numerically evaluated. Due to the internal degrees of freedom (Matsubara frequencies) the quantum version of the LCE is much more complicated than its classical counterpart. We hence cannot expect to go that far in summing various classes of diagrams as in the case of classical fluids or spin systems. In the quantum case we are practically restricted to Φ -derivable approximations [16] where higher order vertices ($n > 2$) are neglected. We therefore resort to LCE diagrams with *renormalized* 1- and 2-vertices only, i.e. to vertices that are at most second derivatives of the renormalized functional g . An approximation for the functional $g^{(N)}$ containing maximally N -vertices can be represented in the Baym form [9]

$$g^{(N)} = \exp \left\{ \sum_{n=1}^N \text{tr} \left[\widehat{C}_n \widehat{\nabla}_x^n \right] \right\} g^{(0)} \{x\} \Big|_{x=0} + \Phi \left[\widehat{\Gamma} \right] - \sum_{n=1}^N \text{tr} \left[\widehat{C}_n \widehat{\Gamma}_n \right], \quad (15)$$

where $\widehat{\Gamma}_n$ is a renormalized n -vertex, \widehat{C}_n is a renormalized n -edge and $\widehat{\nabla}_x$ is a derivative in appropriate generating sources x . Symbols with hats stand for matrices. Here the trace tr is taken over all the internal degrees of freedom. The use of generally renormalized quantities is crucial here, since only then the functions $\widehat{\Gamma}_n$ and \widehat{C}_n can be treated as independent variational variables and the resultant approximation can lead to a thermodynamically consistent and conserving approximation. The matrix variables \widehat{C}_n and $\widehat{\Gamma}_n$ are determined from stationarity equations, i.e. $\delta g^{(N)} / \delta \widehat{\Gamma}_n = \delta g^{(N)} / \delta \widehat{C}_n = 0$.

If we restrict the theory to $N = 2$ we are left with two types of diagrams contributing to Φ . The former is the effective-field contribution involving only Γ_1 . The functional $\Phi^{(1)}$ then takes the form

$$\Phi^{(1)}[\Gamma] = \text{tr} \begin{array}{c} \bullet \\ \vdots \\ \bullet \end{array} = -\frac{U}{2} \sum_{\sigma} \int_0^{\beta} d\tau \frac{\delta g^{(1)}}{\delta \mu_{\sigma}(\tau)} \frac{\delta g^{(1)}}{\delta E_{-\sigma}(\tau)}. \quad (16)$$

Since we expand around a mean field where E_{σ} are variational parameters, the derivative $\delta g^{(1)} / \delta E_{-\sigma} = 0$ for arbitrary $\tau \in [0, \beta]$. The “effective-field” approximation around a mean-field must hence vanish. This is a consequence of stationarity of the mean-field approximation w.r.t. all variables.

A further step and the first nontrivial correction to a MFT within the LCE are the ring diagrams consisting of single loops with only 2-vertices $\widehat{\Gamma}_2$. It is easy to find a diagrammatic representation for the ring diagrams contributing to the functional Φ :

$$\begin{array}{c} \bullet \\ \circ \text{---} \text{---} \text{---} \circ \\ \bullet \end{array} + \frac{1}{2} \begin{array}{c} \bullet \\ \circ \text{---} \text{---} \text{---} \circ \\ \bullet \end{array} + \frac{1}{3} \begin{array}{c} \bullet \\ \circ \text{---} \text{---} \text{---} \circ \\ \bullet \end{array} + \dots$$

To find a mathematical expression for the sum of ring diagrams we must first explicitly write down a matrix representation for both the renormalized vertices (full circles) as well as for the bare edges (dashed lines). They are 4×4 matrices in the case of the strong-coupling MFT and 2×2 matrices in the weak-coupling MFT. In the strong-coupling MFT we denote $\Gamma_{\sigma_1\sigma_2}^{\alpha_1\alpha_2} = \delta^2 g^{(2)} / \delta x_{\sigma_1}^{\alpha_1} \delta x_{\sigma_2}^{\alpha_2}$ and represent the 2-vertex as a matrix

$$\widehat{\Gamma}_2 = \begin{pmatrix} \widehat{\Gamma}_{\sigma\sigma'}^{++} & \widehat{\Gamma}_{\sigma\sigma'}^{+-} \\ \widehat{\Gamma}_{\sigma\sigma'}^{-+} & \widehat{\Gamma}_{\sigma\sigma'}^{--} \end{pmatrix} \quad (17)$$

where the single matrix elements are 2×2 matrices. The bare edge \widehat{v} can be represented as another 4×4 matrix

$$\widehat{v} = \frac{U}{2} \delta(\tau - \tau') \begin{pmatrix} \widehat{0} & \widehat{\sigma}_1 \\ \widehat{\sigma}_1 & \widehat{0} \end{pmatrix}, \quad (18)$$

where $\widehat{\sigma}_1 = \begin{pmatrix} 0 & 1 \\ 1 & 0 \end{pmatrix}$ is the first Pauli matrix. Using this matrix representation we can write down the sum of ring diagrams for the grand potential as

$$\Phi^{(2)}[\widehat{\Gamma}] = -\frac{1}{2} \text{tr} \ln \left(\widehat{1} - \widehat{v} \widehat{\Gamma}_2 \right). \quad (19)$$

The prefactor $1/2$ compensates the doubling of contributions to the grand potential due to the chosen matrix representation. Inserting (19) in (15) we obtain

$$g^{(2)} = \exp \left\{ \frac{1}{2} \text{tr} \left[\widehat{C}_2 \widehat{\nabla}_x^2 \right] \right\} g^{(0)} \{x\} \Big|_{x=0} - \frac{1}{2} \text{tr} \ln \left(\widehat{1} - \widehat{v} \widehat{\Gamma}_2 \right) - \frac{1}{2} \text{tr} \left[\widehat{C}_2 \widehat{\Gamma}_2 \right] \quad (20)$$

where \widehat{C}_2 and $\widehat{\nabla}_x$ are also 4×4 matrices. Approximation (20) was used by Horwitz and Callen [17] and Bloch and Langer [18] to improve the Weiss MFT for the Ising model. Although solvable at the classical level, it is not viable at the quantum level where the generating sources are time dependent. The exponential in (20) leads to a new functional integration being as complicated as in the original problem. We hence have to approximate the exponential. The simplest way to do that is to use the power expansion in \widehat{C}_2 and to terminate it appropriately. Since the most important dynamical fluctuations come from second order perturbation theory, we resort to an approximation reproducing the exact result asymptotically at least to U^2 . A more complete treatment will be presented in Sec. VII.

To reproduce second order of perturbation theory it is sufficient to take into account only the linear term in the operator \widehat{C}_2 . Then (20) reduces to

$$g^{(2)} = g^{(0)} + \frac{1}{2} \text{tr} \left[\widehat{C}_2 \widehat{\nabla}_x^2 \right] g^{(0)} \{x\} \Big|_{x=0} - \frac{1}{2} \text{tr} \ln \left(\widehat{1} - \widehat{v} \widehat{\Gamma}_2 \right) - \frac{1}{2} \text{tr} \left[\widehat{C}_2 \widehat{\Gamma}_2 \right]. \quad (21)$$

Such an approximation is already explicitly solvable and leads to an analytic expression for the grand potential $\Omega^{(2)} = -\beta^{-1} g^{(2)}$. We use the matrix representations for $\widehat{\Gamma}_2$ and \widehat{v} , (17) and (18), and evaluate the second derivative of the unperturbed functional $g^{(0)}$. It immediately follows from (8b) that the derivatives with different spin indices vanish and the matrix of the second derivative in (21) substantially simplifies especially in the frequency representation. Stationarity of the functional $g^{(2)}$ w.r.t. \widehat{C}_2 and $\widehat{\Gamma}_2$ yields explicit expressions for these matrix functions. We exclude them from the potential $g^{(2)}$ and consider the paramagnetic phase exclusively, so that the quantities loose their spin dependencies. We then obtain for the physical grand potential

$$\begin{aligned} \frac{1}{2N} \Omega_{MF}^{(2)} &= -En^s - \beta^{-1} \sum_{n=-\infty}^{\infty} e^{i\omega_n 0^+} \left\{ \int_{-\infty}^{\infty} d\epsilon \rho(\epsilon) \ln [i\omega_n + \mu - E - \Sigma(i\omega_n) - \epsilon] + \ln G(i\omega_n) \right. \\ &+ (1 - n^s) \left[\ln \gamma(i\omega_n) - \beta^{-1} \ln(1 - n^s) \right] + n^s \left[\ln \left[\gamma(i\omega_n) - \frac{U}{2} \right] - \beta^{-1} \ln n^s \right] \left. \right\} \\ &+ \frac{1}{4\beta} \sum_{\alpha=\pm 1} \sum_{m=-\infty}^{\infty} e^{i\nu_m 0^+} \ln \left[1 - \alpha U \left\{ (1 - n^s) \langle G^{(0)} G^{(0)} \rangle (i\nu_m) + n^s \langle G^{(U)} G^{(U)} \rangle (i\nu_m) \right\} \right]. \quad (22) \end{aligned}$$

Here $\omega_n = (2n+1)\pi\beta^{-1}$, $\nu_m = 2m\pi\beta^{-1}$. We further used the abbreviations $\gamma(z) = G(z)^{-1} + \Sigma(z)$, $G^{(0)}(z) = \gamma(z)^{-1}$, $G^{(U)}(z) = \left[\gamma(z) - \frac{U}{2} \right]^{-1}$ and

$$\langle G^{(a)}G^{(a)} \rangle(z) = \beta^{-1} \sum_{n=-\infty}^{\infty} G^{(a)}(i\omega_n)G^{(a)}(z + i\omega_n) \quad (23)$$

with $a = 0, U$. The mean-field parameters E and n^s , and the complex functions $\Sigma(i\omega_n)$ and $G(i\omega_n)$ at fixed μ are treated in the approximate grand potential $\Omega^{(2)}$ variationally in the same way as in the unperturbed theory with $\Omega^{(0)}$. The new grand potential $\Omega^{(2)}$ defines then a thermodynamically consistent theory.

An analogous expression can be derived for the expansion around the weak-coupling MFT. Explicitly we obtain

$$\begin{aligned} \frac{1}{2\mathcal{N}}\Omega_{HF}^{(2)} = & -\frac{U}{2}n^2 - \beta^{-1} \sum_{n=-\infty}^{\infty} e^{i\omega_n 0^+} \left\{ \int_{-\infty}^{\infty} d\epsilon \rho(\epsilon) \ln [i\omega_n + \mu - Un - \Sigma(i\omega_n) - \epsilon] + \ln G(i\omega_n) \right. \\ & \left. + \ln \gamma(i\omega_n) \right\} + \frac{1}{4\beta} \sum_{\alpha=\pm 1} \sum_{m=-\infty}^{\infty} e^{i\nu_m 0^+} \ln \left[1 - \alpha U \langle G^{(0)}G^{(0)} \rangle(i\nu_m) \right] \end{aligned} \quad (24)$$

where the function $G^{(0)}$ has the same meaning as in (22). Grand potentials (22) and (24) hold only for the paramagnetic phase. Grand potentials allowing for a broken symmetry can be derived without conceptual changes.

Having explicit expressions for the contributions due to the ring diagrams we can compare the resulting theory with other similar approximate schemes, especially those studied extensively by Menge and Müller-Hartmann [19], iterated perturbation theory (IPT) introduced recently [10,20,21] in connection with the metal-insulator transition in the $d = \infty$ Hubbard model, and with the extended Edwards-Hertz approximation [22,23]. This will be done in Secs. VI and VII. Before we do this we should realize that the presented sum of diagrams within the LCE scheme does not renormalize the one-electron Green function but rather the interaction strength. The ring-diagram approximation (22), (24) represents a sum of a geometric series of 2-particle bubbles renormalizing the interaction, i.e. diagrams contributing to the polarization of the vacuum. Because of the locality of the electron-electron interaction in the Hubbard model only even powers of U contribute. Grand potentials (22), (24) correspond to an ‘‘effective-interaction’’ (bubble-chain) approximation studied at the level of self-energy in [19]. However, the derived sum of ring diagrams does not represent a fully self-consistent approximation, since the local electron propagators in the expansion are unrenormalized, mean-field ones, $G^{(0)}, G^{(U)}$. Although these propagators contain the self-energy Σ and are not free, the dependence of $G^{(a)}$ on Σ is caused by the reduction of a $d = \infty$ theory to a $d = 0$ (single-site) problem. Such a partial self-consistency is of topological rather than of dynamical origin. Moreover, neither (22) nor (24) has the Baym form [5] where the Φ -functional depends only on the full propagator G . We hence have no guarantee that they are conserving approximations.

V. ONE-PARTICLE PROPERTIES

Grand potential (22) leads to a numerically solvable theory. In the present form it is only suitable for the paramagnetic phase and we use it to evaluate explicitly the one-electron properties. In order to simplify the numerical procedure we restrict our considerations to zero temperature.

The defining equations for the variational variables are derived from stationarity of $\Omega^{(2)}$. Vanishing of the derivatives w.r.t. the static variables n^s and E leads to

$$E = \mathcal{E} + \frac{U}{4\beta} \sum_{m=-\infty}^{\infty} e^{i\nu_m 0^+} \sum_{\alpha=\pm 1} \alpha C_{\alpha}(i\nu_m) \left[\langle G^{(0)}G^{(0)} \rangle(i\nu_m) - \langle G^{(U)}G^{(U)} \rangle(i\nu_m) \right], \quad (25a)$$

$$n^s = \beta^{-1} \sum_{n=-\infty}^{\infty} e^{i\omega_n 0^+} \int_{-\infty}^{\infty} d\epsilon \rho(\epsilon) [i\omega_n + \mu - E - \Sigma(i\omega_n) - \epsilon]^{-1}, \quad (25b)$$

where

$$\mathcal{E} = -\beta^{-1} \sum_{n=-\infty}^{\infty} e^{i\omega_n 0^+} \ln \left[1 - \frac{U}{2} G^{(0)}(i\omega_n) \right] \quad (25c)$$

and

$$C_\alpha(z) = \left[1 - \alpha U \left\{ (1 - n^s) \langle G^{(0)} G^{(0)} \rangle (z) + n^s \langle G^{(U)} G^{(U)} \rangle (z) \right\} \right]^{-1}. \quad (25d)$$

The term in (25a) including a sum over bosonic frequencies is a correction to the unperturbed static MFT due to the ring diagrams. Variations of $\Omega^{(2)}$ w.r.t. $\Sigma(i\omega_n)$ and $G(i\omega_n)$ lead to corrected mean-field equations for these functions:

$$G(i\omega_n) = \int_{-\infty}^{\infty} d\epsilon \rho(\epsilon) [i\omega_n + \mu - E - \Sigma(i\omega_n) - \epsilon]^{-1} \quad (26a)$$

and

$$\begin{aligned} G(i\omega_n) &= (1 - n^s) G^{(0)}(i\omega_n) + n^s G^{(U)}(i\omega_n) \\ &\quad - \frac{U}{4\beta} (1 - n^s) G^{(0)}(i\omega_n)^2 \sum_{\alpha=\pm 1} \alpha \sum_{m=-\infty}^{\infty} e^{i\nu_m 0^+} G^{(0)}(i\omega_n + i\nu_m) [C_\alpha(i\nu_m) + C_\alpha(-i\nu_m)] \\ &\quad - \frac{U}{4\beta} n^s G^{(U)}(i\omega_n)^2 \sum_{\alpha=\pm 1} \alpha \sum_{m=-\infty}^{\infty} e^{i\nu_m 0^+} G^{(U)}(i\omega_n + i\nu_m) [C_\alpha(i\nu_m) + C_\alpha(-i\nu_m)]. \end{aligned} \quad (26b)$$

To facilitate the numerical evaluation of the derived equations we convert the sums over Matsubara frequencies to integrals over real frequencies. However, this is possible only if the functions under consideration are analytic in the upper and lower complex half-planes. Apart from the one-particle Green function, the analytic structure of which is clear, there are two other complex functions $\langle G^{(a)} G^{(a)} \rangle (z)$ and $C_\alpha(z)$. The former function is analytic with a cut along the real axis as can be seen from the representation

$$X^{(a)}(z) := \langle G^{(a)} G^{(a)} \rangle (z) = -\frac{1}{\pi} \int_{-\infty}^0 dx \left[G^{(a)}(x+z) + G^{(a)}(x-z) \right] \text{Im} G^{(a)}(x+i0^+). \quad (27)$$

On the other hand the function $C_\alpha(z)$ can have a pole in the complex plane if

$$1 = \alpha U \left\{ (1 - n^s) X^0(z) + n^s X^{(U)}(z) \right\}. \quad (28)$$

Since $X^{(a)}(z) = X^{(a)}(-z)$, the r.h.s. of (28) is real for $z = iy$, i.e. along the imaginary axis. There may be a critical value U_c at which the pole appears for the first time at $z = 0$ and where the perturbation expansion breaks down. We must hence distinguish two regimes of the interaction strength. If $U < U_c$ (weak coupling) we have no polar contributions to the spectral representations of the Matsubara sums. At strong coupling, $U > U_c$, the pole in $C_\alpha(z)$ influences the integrals over real frequencies. The existence of a pole in a two-particle Green function indicates an instability of perturbation theory and is connected with a metal-insulator transition. We postpone a detailed investigation of the actual role of such a pole to a separate publication and stick in this paper exclusively to the weak-coupling regime $U < U_c$. In this case it is easy to show that the sum over bosonic frequencies in (25a) vanishes due to analyticity of the integrand in the upper and lower complex half-planes. Therefore the mean-field equations for n^s and E are not changed by the contributions from the ring diagrams. Eq. (26b) can be rewritten at weak coupling for an arbitrary complex energy z as

$$G(z) = (1 - n^s) G^{(0)}(z) \left\{ 1 + \frac{U}{2} G^{(0)}(z) I^{(0)}(z) \right\} + n^s G^{(U)}(z) \left\{ 1 + \frac{U}{2} G^{(U)}(z) I^{(U)}(z) \right\}, \quad (29a)$$

where we used

$$I^{(a)}(z) = \sum_{\alpha=\pm 1} \frac{\alpha}{\pi} \int_{-\infty}^0 dx \left[C_\alpha(z-x) \text{Im} G^{(a)}(x+i0^+) - G^{(a)}(z+x) \text{Im} C_\alpha(-x+i0^+) \right]. \quad (29b)$$

The function $C_\alpha(z)$ is defined through the functions $X^{(a)}$ as

$$C_\alpha(z) = \left\{ 1 - \alpha U \left[(1 - n^s) X^{(0)}(z) + n^s X^{(U)}(z) \right] \right\}^{-1}. \quad (30)$$

Equation (29a) can be turned into an equation for the self-energy $\Sigma(z)$ if we use the definition of $G^{(a)}$ given below eq. (22). We then obtain

$$\begin{aligned} \Sigma(z) = & \frac{U}{2} \frac{n^s}{1 + G(z) [\Sigma(z) - U/2]} \left\{ 1 + \frac{1 + G(z)\Sigma(z)}{1 + G(z) [\Sigma(z) - U/2]} I^{(U)}(z) \right\} \\ & + \frac{U}{2} \frac{1 - n^s}{1 + G(z)\Sigma(z)} I^{(0)}(z). \end{aligned} \quad (31)$$

Eq. (31), completed with the mean-field equations

$$E = \frac{1}{\pi} \int_{-\infty}^0 dx \text{Im} \ln \left[1 - \frac{U}{2} G^{(0)}(x + i0^+) \right] \quad (32a)$$

and

$$n^s = -\frac{1}{\pi} \int_{-\infty}^0 dx \text{Im} G(x + i0^+), \quad (32b)$$

is to be solved numerically for $z = \omega + i0^+$. From (32b) we see that $n^s = n$ as is the case in the static MFT from [6]. Due to the electron-hole symmetry it is sufficient to solve the equations for $\omega \leq 0$. To obtain the values for the self-energy and the one-electron Green function on the positive frequency axis we use the electron-hole transformation ($n \rightarrow 1 - n, \omega \rightarrow -\omega$) leading to:

$$G(-\omega + i0^+) = -G(\omega + i0^+)^* \quad (33a)$$

and

$$\Sigma(-\omega + i0^+) = \frac{U}{2} - \Sigma(\omega + i0^+)^*. \quad (33b)$$

The chemical potential transforms in this expansion as $\mu \rightarrow U/2 - \mu$ and the parameter $E \rightarrow -E$. It is to be proved that (33) really holds for a solution of (31), i.e. the approximate theory correctly exhibits the electron-hole symmetry. The proof is presented in the Appendix.

The same steps can be made to derive equations for the self-energy of the ring diagrams summed around the Hartree-Fock grand potential (24). The resulting self-energy then is

$$\Sigma_{HF}(z) = \frac{U/2}{1 + G(z)\Sigma(z)} I^{(0)}(z). \quad (34)$$

We see that the self-energy from the strong-coupling MFT formally reduces to Σ_{HF} if we put $n^s = 0$ and $E = Un$.

The electron-hole symmetry in the weak-coupling case takes the form

$$G(-\omega + i0^+) = -G(\omega + i0^+)^*, \quad (35a)$$

$$\Sigma_{HF}(-\omega + i0^+) = -\Sigma_{HF}(\omega + i0^+)^*. \quad (35b)$$

VI. NUMERICAL RESULTS AND COMPARISON OF VARIOUS APPROXIMATE SCHEMES

We now apply the derived equations in the weak-coupling limit to assess quantum fluctuations due to dynamical corrections to the static MFT. Only for the sake of simplicity we perform the numerical calculations on a Bethe lattice in $d = \infty$, i.e. we use for the diagonal element of the one-electron Green function the representation

$$G^{(0)}(z) = \left[z - \frac{D^2}{4} G(z) \right]^{-1} \quad (36)$$

where $D = 2$ equals half the bandwidth. We also restrict the calculation to the half-filled band in the paramagnetic phase, i.e. $n_\sigma = n_\sigma^s = 1/2$ and $\mu = U/4$ ($\mu - E = 0$). Furthermore we remain during all the calculations at $T = 0$.

Since our aim is to investigate the resulting equations only in the weak-coupling limit, we separately analyze the U^2 corrections to the static MFT before we take into account all the ring diagrams. In course of calculations we compare the results obtained from the LCE treated here with other approximations of similar origin.

A. U^2 -corrections to the mean-field solutions

Let us start with the simpler expansion around the Hartree-Fock MFT. Using (34) we obtain for the U^2 -contributions to the self-energy

$$\begin{aligned} \Sigma(z) = \frac{U^2}{1 + G(z)\Sigma(z)} I_0^{(0)}(z) \equiv \frac{U^2}{1 + G(z)\Sigma(z)} \int_{-\infty}^0 \frac{dx}{\pi} \left[X^{(0)}(z-x) \text{Im}G^{(0)}(x+i0^+) \right. \\ \left. + G^{(0)}(z+x) \text{Im}X^{(0)}(x+i0^+) \right]. \end{aligned} \quad (37)$$

The resulting self-energy consists of two different contributions, the algebraic prefactor and the integral $I_0^{(0)}$. The former is a consequence of the incomplete self-consistency of the defining equation (37). The Green function $G^{(0)}$ from the r.h.s. of (37) is not identical with the full one-electron propagator G . Hence the variation of the grand potential (22) w.r.t. G , leading to the equation for the self-energy, generates algebraic factors due to the variation of the propagator $G^{(0)}$. The latter contribution to (37) is exactly the result of the iterated perturbation theory (IPT) and corresponds to a partially self-consistent, second-order Feynman diagram for the self-energy. It is important that both the contributions are complex and lead to a rather intricate analytic structure of the self-energy $\Sigma(z)$. It is impossible to prove the desired Herglotz properties, i.e. $\Sigma(z) = \Sigma(z^*)^*$ and $\text{Im}\Sigma(z) \propto -\text{Im}z$ for all complex energies z . Only at the Fermi level, $\omega = 0$, we obtain from the electron-hole symmetry that $\Sigma(0) = 0$.

Approximation (37) does not seem to cause troubles at weak coupling ($U \leq 1.9$), where only a slight modification of the non-interacting density of states (DOS) can be observed (Fig. 1). However, interactions stronger than $U_c \approx 1.9$ lead to a breakdown of the approximate equations, since a singularity appears in the prefactor $[1 + G(z)\Sigma(z)]^{-1}$. Namely we observe that the derivative $\partial G^{(0)}(\omega)/\partial\omega$ diverges at a critical frequency ω_c , which leads to a jump in the propagator $G^{(0)}(\omega)$. The density of states then develops a cusp at the critical frequencies $\pm\omega_c$ (Fig. 2). In such a situation it is impossible to reach convergence and it is unclear if the equation (37) does have a solution at all.

The algebraic prefactor is a consequence of the variation of the grand potential and has no diagrammatic background. It causes the breakdown of the iteration scheme. We may ask if we can do better by neglecting this prefactor. Such a choice corresponds to the diagrammatic expansion directly applied to the self-energy instead of to the grand potential. We obtain

$$\Sigma(z) = U^2 \int_{-\infty}^0 \frac{dx}{\pi} \left[X^{(0)}(z-x) \text{Im}G^{(0)}(x+i0^+) + G^{(0)}(z+x) \text{Im}X^{(0)}(x+i0^+) \right], \quad (38)$$

which is the IPT self-energy. Analyzing (38) we find that this equation can safely be iterated up to $U \approx 4.7$ (Fig. 3) where the results of Georges and Krauth [21] are reproduced. The DOS shows a three-peak structure where the central band narrows with increasing U . However, it seems impossible to reach the alleged metal-insulator transition at which the width of the middle band has to vanish. Before we reach this point, the iterations break down for similar reasons as in the solution of (37). With increasing interaction strength a discontinuity in the real part of the Green function $G^{(0)}(\omega)$ seems to develop together with a cusp in its imaginary part (Figs. 4a, b). The extremal points for both the functions approach each other (Fig. 5) and seem to merge at $\omega_c < 0$, i.e. away from the Fermi energy. Earlier a singularity in $G^{(0)}$ was reported on the real axis only at the Fermi energy [20]. According to our results the Green function $G^{(0)}$ displays a discontinuity at ω_c and it is again impossible to reach a solution via iterations. If we attempt to solve (38) for complex energies, the breakdown of the iteration scheme is shifted to stronger interactions and the critical frequency is pushed towards the Fermi energy. Although the singularity smooths in comparison with the real frequencies, we did not succeed to remove it completely from $G^{(0)}$ and to reach a convergent solution at strong coupling. If there were a singularity at $G^{(0)}$ even at complex frequencies, the Green function could not fulfil the desired Herglotz properties. However, if the Herglotz properties of $G^{(0)}(z)$ were violated, it would be impossible to continue analytically the quantities from the imaginary frequency axis to the real energies in a unique way. The approximation then would become unreliable with possible spurious poles (zeros) in the complex plane. It is hence of great importance now to prove or disprove the Herglotz properties of the IPT self-energy if we want to draw conclusions from this approximation especially at strong coupling.

From the above results it may seem that the IPT for the self-energy be superior to the LCE for the grand potential because of the unphysical complex prefactor in (37). This prefactor appears due to the fact that the one-electron propagator $G^{(0)}$, used in the ring diagrams, deviates from the full propagator G and thus the expansion is not fully self-consistent. It is a consequence of the non-self-consistent character of the expansion that not all physical quantities have a diagrammatic expansion. Diagrammatically the derivative is not connected with a cut of the one-electron

propagator only, but a variation of $G^{(0)}$ w.r.t. G appears. This variation leads to the loss of the diagrammatic control over physical quantities and causes violation of Ward identities. Undesired prefactors are inevitable companions of non- or only partly self-consistent theories. Although nonexistent at the level of self-energy within the IPT, the unphysical prefactors do appear in higher order Green functions and correlation functions (susceptibilities). Therefore we cannot rely on IPT susceptibilities [21]. Since the existence of “spurious” complex prefactors is a ubiquitous feature of partly self-consistent theories, we may conclude that only fully self-consistent theories in the spirit of Baym offer a physically consistent global picture.

We can also calculate the U^2 corrections to the strong-coupling MFT. There we meet the same problems with prefactors and a breakdown of the iteration scheme as in the case of the expansion around the Hartree-Fock MFT.

B. Corrections to the mean-field solutions due to the ring diagrams

One may still hope to improve the weak-coupling approximation and to avoid the breakdown of the iteration scheme by taking into account the ring diagrams. However, the theory with ring diagrams suffers from the same deficiency as the U^2 terms, namely the equations contain unphysical complex prefactors, and an analogous breakdown of the iteration procedure is to be expected. It turns out that for the ring diagrams a singularity in the prefactor $[1 + G(z)\Sigma(z)]^{-1}$ shows up even for smaller values of the interaction, namely $U \approx 1.66$, where the approximation scheme breaks down. Above this value the iterations do not converge any longer. It indicates that the additive diagrams push down the “transition” from the weak to the strong coupling regimes. To confirm this we suppressed the prefactors and thus gained an extension of the self-energy from the IPT (38) due to the ring diagrams. The result is plotted in Fig. 6. We can see that the self-energy has a narrow central peak with a tendency to build up two satellite bands. However, before the satellites can be fully formed a pole in the two-particle function $C_\alpha(\omega)$ (30) at $\omega = 0$ is reached at $U \approx 1.9$ and the theory breaks down. There is no way to go around the pole in the two-particle function $C_\alpha(z)$ in this not fully self-consistent approximation. The pole causes the Herglotz properties to be manifestly broken. There is no convergent solution for $U > 1.9$. The only way to restore analytic properties of the local, one-electron Green function is to make the theory fully self-consistent.

VII. SELF-CONSISTENCIES AND RENORMALIZATIONS IN THE LINKED CLUSTER EXPANSION

We saw in the preceding section that non-self-consistent diagrammatic approximations lead to differences in physical quantities derived either diagrammatically or with the use of derivatives (variations) of the grand potential w.r.t. external sources. This is a general feature of not fully self-consistent approximations where some Ward identities are violated. This conclusion applies also to the approximations investigated in Secs. IV-VI. Although the corresponding grand potential has a form where all the unknown functions have to be determined from stationarity conditions, the internal electron propagators in the diagrams are $G^{(0)} = (G^{-1} + \Sigma)^{-1}$ (or $G^{(U)} = (G^{-1} + \Sigma - U/2)^{-1}$) instead of G as one expects in the Baym approach. These are dynamically free propagators, since the dependence on the self-energy does not stem from the dynamics but rather from a special topology of the $d = \infty$ lattice mapped onto a single site (impurity) embedded in a medium. E.g. if the diagrams were treated in $d = 3$, the function $G^{(0)}(z)$ had to be replaced by the bare (unperturbed) \mathbf{k} -dependent propagator $G^{(0)}(\mathbf{k}, z)$. There would be no self-consistency at all in finite dimensional lattices. The origin of the partial self-consistency in the investigated approximate schemes lies entirely in the reduction of the topology of the $d = \infty$ model to a “self-consistent” single-site problem [24]. The topological self-consistency in the local propagator $G^{(0)}(z)$ coherently copies the dynamical processes from the impurity to the medium which, on the other hand, provides the electrons for the impurity.

In this light it is clear that e.g. the self-energy, obtained by varying the grand potential from the LCE, does not equal the self-energy obtained from a sum of the non-self-consistent self-energy diagrams. To get rid of such ambiguity problems we must abandon non-self-consistent theories and introduce true dynamical renormalizations into the LCE. We can try to introduce the self-consistency naively via a replacement of the unperturbed electron propagator $G^{(0)}$ with the full propagator G . However, such an introduction of the self-consistency into the theory is dangerous, since it need not be diagrammatically controlled. This naive way of turning the theory self-consistent may lead to multiple counting of diagrams and to undesired unphysical and spurious structures. The only consistent way to introduce self-consistencies into diagrammatic expansions is to classify diagrams into particular classes which may be summed by iterations, i.e. by self-similar insertions.

Possible renormalization schemes within the LCE were extensively discussed by Wortis [9]. However, in the quantum case with internal time (frequency) degrees of freedom, we are much more restricted to produce a tractable approximation. As we already mentioned, even a quantum analogue of the Bloch-Langer approximation from the classical

Heisenberg model [18] is not viable in the quantum case. Due to the time dependence of the vertices the ordering of functional derivatives, i.e. the time ordering of the external legs at vertices, is important. Interchange of derivatives leads to “crossing” of interaction lines and to different quantitative results for diagrams with vertices of higher order than two. If we resort to a fixed time ordering of the vertex legs, i.e. to a kind of “noncrossing approximation” we obtain a self-consistent version of the ring-diagram approximation.

To this end we must take into account noncrossing diagrams resulting from the expansion of the exponential $\exp\left\{\frac{1}{2}\text{tr}\left[\widehat{C}_2\widehat{V}_x^2\right]\right\}$ in (20). If we analyze the contributions from products of the operator $\widehat{C}_2\widehat{V}_x^2$ we can classify them into crossing and noncrossing diagrams, according to whether the two-point function C_2 is or is not crossed by an interaction line (Fig. 8), respectively. The topology of higher order diagrams becomes more and more intricate due to the crossed diagrams (Fig. 8d). If we neglect them we can exactly sum up the contributions from the noncrossing diagrams via self-consistency. Insertions as in Fig. 8c can be summed by replacing $G^{(0)}$ with \overline{G} , where the self-energy due to the C -contributions (hatched bubbles) equals to a convolution $\overline{G} * C$. The grand potential due to the self-consistent ring diagrams around the Hartree-Fock MFT can then be written as a generating Baym functional

$$\begin{aligned} \frac{1}{\mathcal{N}}\Omega_{HF}^{(ring)} = & -Un_{\uparrow}n_{\downarrow} - \beta^{-1} \sum_{\sigma} \sum_{n=-\infty}^{\infty} e^{i\omega_n 0^+} \left\{ \int_{-\infty}^{\infty} d\epsilon \rho(\epsilon) \ln [i\omega_n + \mu - Un_{-\sigma} - \Sigma_{\sigma}(i\omega_n) \right. \\ & - \Delta\Sigma_{\sigma}(i\omega_n) - \epsilon] + \Delta\Sigma_{\sigma}(i\omega_n)\overline{G}_{\sigma}(i\omega_n) + \ln [1 + G_{\sigma}(i\omega_n) (\Sigma_{\sigma}(i\omega_n) - \langle\overline{G}_{\sigma}C_{\sigma}\rangle(i\omega_n))] \left. \right\} \\ & + \beta^{-1} \sum_{m=-\infty}^{\infty} e^{i\nu_m 0^+} \left\{ \sum_{\sigma} \Gamma_{\sigma}(i\nu_m)C_{\sigma}(i\nu_m) + \frac{1}{2} \ln [1 - U^2\Gamma_{\uparrow}(i\nu_m)\Gamma_{\downarrow}(i\nu_m)] \right\} \end{aligned} \quad (39)$$

where we used the same notation for the convolution $\langle\overline{G}_{\sigma}C_{\sigma}\rangle(i\omega_n)$ as in (23), but with the sum over bosonic Matsubara frequencies. Here $\Delta\Sigma_{\sigma}$ is a correction due to the C_{σ} -induced contributions from the noncrossing diagrams and \overline{G}_{σ} is its Legendre conjugate variable. If they vanish, (39) reduces to its non-self-consistent version (24). If we exclude the variables Γ_{σ} , C_{σ} and \overline{G}_{σ} , $\Delta\Sigma_{\sigma}$ we can reduce (39) at the saddle point to

$$\begin{aligned} \frac{1}{\mathcal{N}}\Omega_{HF}^{(ring)} = & -Un_{\uparrow}n_{\downarrow} - \beta^{-1} \sum_{\sigma} \sum_{n=-\infty}^{\infty} e^{i\omega_n 0^+} \left\{ \int_{-\infty}^{\infty} d\epsilon \rho(\epsilon) \ln [i\omega_n + \mu - Un_{-\sigma} - \Sigma_{\sigma}(i\omega_n) - \epsilon] \right. \\ & \left. + G_{\sigma}(i\omega_n)\Sigma_{\sigma}(i\omega_n) \right\} + \frac{1}{2\beta} \sum_{m=-\infty}^{\infty} e^{i\nu_m 0^+} \ln [1 - U^2\langle G_{\uparrow}G_{\uparrow}\rangle(i\nu_m)\langle G_{\downarrow}G_{\downarrow}\rangle(i\nu_m)] . \end{aligned} \quad (40)$$

Grand potential $\Omega_{HF}^{(ring)}$ is the fully self-consistent “bubble-chain” approximation investigated at the level of self-energy by Menge and Müller-Hartmann [19].

Analogously to (39) we derive a self-consistent version of the ring-diagram grand potential for the LCE around the strong-coupling MFT:

$$\begin{aligned} \frac{1}{\mathcal{N}}\Omega_{MF}^{(ring)} = & -\beta^{-1} \sum_{\sigma} \sum_{n=-\infty}^{\infty} e^{i\omega_n 0^+} \left\{ \int_{-\infty}^{\infty} d\epsilon \rho(\epsilon) \ln [i\omega_n + \mu - E_{\sigma} - \Sigma_{\sigma}(i\omega_n) - \Delta\Sigma_{\sigma}(i\omega_n) - \epsilon] \right. \\ & + (1 - n_{-\sigma}^s) \ln [1 + G_{\sigma}(i\omega_n) (\Sigma_{\sigma}(i\omega_n) - \langle\overline{G}_{\sigma}C_{\sigma}\rangle(i\omega_n))] + \Delta\Sigma_{\sigma}(i\omega_n)\overline{G}_{\sigma}(i\omega_n) \\ & \left. + n_{-\sigma}^s \ln \left[1 + G_{\sigma}(i\omega_n) \left(\Sigma_{\sigma}(i\omega_n) - \frac{U}{2} - \langle\overline{G}_{\sigma}C_{\sigma}\rangle(i\omega_n) \right) \right] \right\} - \sum_{\sigma} E_{\sigma}n_{\sigma}^s \\ & + \beta^{-1} \sum_{m=-\infty}^{\infty} e^{i\nu_m 0^+} \left\{ \sum_{\sigma} \Gamma_{\sigma}(i\nu_m)C_{\sigma}(i\nu_m) + \frac{1}{2} \ln [1 - U^2\Gamma_{\uparrow}(i\nu_m)\Gamma_{\downarrow}(i\nu_m)] \right\} . \end{aligned} \quad (41)$$

Excluding the variables Γ_{σ} and C_{σ} at the saddle point we obtain defining equations for the Green functions G_{σ} and \overline{G}_{σ}

$$\overline{G}_{\sigma}(i\omega_n) = G_{\sigma}(i\omega_n) = \int_{-\infty}^{\infty} d\epsilon \rho(\epsilon) \frac{1}{i\omega_n + \mu - E_{\sigma} - \Sigma_{\sigma}(i\omega_n) - \Delta\Sigma_{\sigma}(i\omega_n) - \epsilon} \quad (42a)$$

and for the self-energies $\Sigma_{\sigma}(i\omega_n)$ and $\Delta\Sigma_{\sigma}(i\omega_n)$

$$\Delta\Sigma_\sigma(i\omega_n) = -\frac{U^2}{2\beta} \sum_{m=-\infty}^{\infty} G_\sigma(i\omega_n + i\nu_m) \frac{\langle G_{-\sigma} G_{-\sigma} \rangle(i\nu_m)}{1 - U^2 \langle G_\uparrow G_\uparrow \rangle(i\nu_m) \langle G_\downarrow G_\downarrow \rangle(i\nu_m)}, \quad (42b)$$

$$\Sigma_\sigma(i\omega_n) - \Delta\Sigma_\sigma(i\omega_n) = \frac{U}{2} \frac{n_\sigma^s}{1 + G_\sigma(i\omega_n) (\Sigma_\sigma(i\omega_n) - \Delta\Sigma_\sigma(i\omega_n) - U/2)}. \quad (42c)$$

Grand potential $\Omega_{MF}^{(ring)}$ has an attractive feature in that it contains the split-band limit of the Hubbard-III solution and is exact at weak coupling up to U^2 . In contrast to previously studied theories with analogous properties [22,23], grand potential (41) is derived in a fully controlled manner. There are no spurious prefactors in the defining equations for the self-energies calculated from (39) and (41). There is also no artificial breakdown of the iteration scheme in the fully self-consistent theory. All the Ward identities are now fulfilled and there is no difference in deriving various physical quantities either from varying the grand potential or using the corresponding diagrammatic expansion for them, since the theory is thermodynamically consistent and conserving in the Baym sense.

We can now analytically continue the functions Σ_σ , $\Delta\Sigma_\sigma$ and G_σ to the whole complex plane and use spectral representations with real frequencies. The numerical solution is then obtained straightforwardly. The quantitative results in the paramagnetic phase (Fig. 8) obtained from (40) at weak coupling ($U \leq 3.5$) agree with the results of the ‘‘bubble-chain’’ approximation from [19]. For stronger coupling a pole in the two-particle function $C_\sigma(\omega)$ interferes and the iteration scheme must be modified to preserve the Herglotz properties of the one-electron propagator [25].

Self-consistent mean-field theory with dynamical fluctuations (42) exhibits similar behavior at weak coupling ($U \leq 1.5$) (Fig. 9). The DOS at the Fermi energy begins to decrease, since the theory is not a Fermi liquid (the term proportional to U^3 violates the Luttinger theorem). Two satellite peaks start to develop and split off at about $U_c \approx 5.5$ ($U_c = 4$ for the static MFT) similarly to [23]. Because of frequency convolutions there are no sharp (algebraic) band edges and it is numerically hard to determine when exactly the bands split off. We also had troubles to reach convergence for the frequencies lying within the expected gap. To reach a reliable solution in the insulating phase, the iteration scheme must be refined. We, however, did not meet any singularities indicating an instability of this dynamical mean-field theory. The two-particle function $C_\sigma(\omega)$ did not reach the pole (28) because of the metal-insulator transition and we did not observe any indication for a divergency in the perturbation theory.

The self-energy from (42) contains two parts, $\Delta\Sigma$ being the direct contribution of the ring diagrams and $\Sigma - \Delta\Sigma$ which is the mean-field self-energy with the renormalized one-electron propagator. To assess these two different self-energies we plotted their imaginary parts separately in Figs. 10a, b and compared them with the corresponding self-energies from the Hartree-Fock solution (40) and the static MFT [14], respectively. We can see that the self-energy $\Delta\Sigma$ from (42) is smoother than in the weak-coupling theory, since the imaginary part of the total self-energy does not vanish at the Fermi energy. The mean-field self-energy $\Sigma - \Delta\Sigma$ is dominant in the vicinity of the Fermi energy, while $\Delta\Sigma$, due to the ring diagrams, is responsible for the band tails.

VIII. CONCLUSIONS

In this paper we derived a general expansion scheme around mean-field theories for interacting electrons. We used a quantum version of the linked cluster expansion modified for the needs of perturbing the mean-field theories under consideration. We used the difference of the full and the mean-field Hamiltonian as the perturbation generating the LCE. We succeeded in this way to put expansions around weak-coupling (Hartree-Fock) and strong-coupling (Hubbard-III) mean-field theories on the same footing. Moreover, the proposed expansion scheme applies to the grand potential (free energy) and hence the self-consistent theory has a variational character and is thermodynamically consistent and conserving in the Baym sense. The presented application of the LCE around mean fields enables to systematically classify, renormalize and sum various classes of diagrams as is usual in the weak-coupling expansion, although the Wick theorem and the Gaussian integration are not used.

We explicitly investigated an approximation using a sum of the so-called ring diagrams leading at the classical level to the Bloch-Langer approximation [18]. We showed that this approximation at the quantum level, where additive internal degrees of freedom represented by Matsubara frequencies are to be involved, is not solvable. Further approximations are enforced to obtain the grand potential in closed form. We discussed and compared various approximations resulting from simplifications of the complete, renormalized sum of the ring diagrams. Thereby we paid special attention to the problem of renormalizations and the self-consistency of the derived approximate solutions.

At first we studied the influence of dynamical fluctuations due to the U^2 term. When expanded around the Hartree-Fock solution, we obtained a modified iterated perturbation theory of [10]. The difference to the IPT was manifested by a complex prefactor in the self-energy. This prefactor is a consequence of a partial self-consistency of

the approximation and of the fact that the LCE is a diagrammatic expansion for the grand potential, whereas the IPT for the self-energy. These prefactors are ubiquitous feature of non-self-consistent or only partially self-consistent theories, where the Ward identities and sum rules need not be fulfilled. Although there are no unphysical complex prefactors in the IPT for the self-energy, the simple analytic structure of e.g. susceptibilities goes lost. There is no set of diagrams generating susceptibilities in the IPT. We found that incompletely self-consistent theories containing the U^2 term break down numerically at a critical U_c above which no stable numerical solution for complex energies was found. This situation did not improve even if we took into account the ring diagrams without any dynamical renormalizations. A pole in the two-particle function destroys convergence of the iterations.

We concluded from the difficulties with nonrenormalized partial summations of the LCE that only dynamically renormalized, fully self-consistent theories can provide global, thermodynamically consistent approximations. We hence developed a scheme how to introduce full self-consistency into the LCE in a controlled and systematic way. We demonstrated the method on an example of the ring diagrams, where we showed that a class of “noncrossing diagrams”, when summed, leads to full self-consistency of the approximation. Such a fully self-consistent theory has a diagrammatic expansion for any derivative of the free energy. The self-consistent version of the ring diagrams around the Hartree-Fock solution was identified with the bubble-chain approximation studied at the level of the self-energy in [19]. We studied approximations with the self-consistent ring diagrams for both the weak and strong coupling mean-field theories. In the weak-coupling case we found that for intermediate interaction strengths a pole in the two-particle function interferes and hinders to reach convergence of iterations. A more advanced approach to handle the behavior of the iterations in the vicinity of the pole must be used to decide how the pole is being approached. This problem, tightly connected with the metal-insulator transition, will be discussed in a separate publication. The ring-diagram approximation around the strong-coupling MFT was found to be stable for all interaction strengths and to lead to a metal-insulator transition at about $U_c \simeq 5.5$ in the same way as the static MFT of [6].

The linked cluster expansion with dynamical renormalizations introduced in this paper is not only suitable to derive conserving approximations with dynamical fluctuations beyond static mean-field theories, but it may prove efficient for expansions around other nontrivial solutions such as the expansion for the Kondo model proposed earlier by Anderson and Yuval [26].

We thank D.Vollhardt for useful discussions. The work was supported in part by the grant No. 202/95/0008 of the Grant Agency of the Czech Republic and by the Sonderforschungsbereich 341 of the Deutsche Forschungsgemeinschaft.

APPENDIX A: ELECTRON-HOLE SYMMETRY

We now prove that the Green function $G(z)$ and consequently the self-energy $\Sigma(z)$ transform under the electron-hole transformation defined as

$$z \rightarrow -z \quad n_\sigma \rightarrow 1 - n_{-\sigma} \quad (\text{A1})$$

according to formulas (33).

We use the results of the static mean-field theory [14] and the fact that the ring diagrams do not change the equations for the mean-field parameters n^s and E to obtain the transformation rules

$$n_\sigma^s \rightarrow 1 - n_{-\sigma}^s, \quad \mu \rightarrow \frac{U}{2} - \mu, \quad E \rightarrow -E. \quad (\text{A2})$$

Note that here we have to replace the interaction strength U from [14] with $U/2$ in the transformation formulas, since we use the convention $\lambda_\sigma = 1/2$, $\lambda_{at} = 0$ instead of $\lambda_\sigma = 1$, $\lambda_{at} = -1$.

To prove the electron-hole symmetry of the ring-diagram approximation we assume the validity of (33) and derive transformations for the functions $G^{(0)}(z)$ and $G^{(U)}(z)$ and the integrals $I^{(0)}(z)$ and $I^{(U)}(z)$ and then insert them into the r.h.s. of (29a) to show that the left as well as the right hand side transform identically.

Using the definitions in eqs. (22), (26a), and (33) we easily obtain

$$G^{(0)}(z) \rightarrow -G^{(U)}(-z), \quad G^{(U)}(z) \rightarrow -G^{(0)}(-z). \quad (\text{A3})$$

Further we must find transformation rules for the integrals $I^{(a)}(z)$. If we extend the integration in these integrals onto the whole real axis we obtain

$$\begin{aligned} & \sum_\alpha \frac{\alpha}{2\pi i} \int_{-\infty}^{\infty} dx \left\{ C_\alpha(z-x) \left[G^{(a)}(x+i0^+) - G^{(a)}(x-i0^+) \right] \right. \\ & \left. + G^{(a)}(z+x) \left[C_\alpha(-x+i0^+) - C_\alpha(-x-i0^+) \right] \right\} = 0, \end{aligned} \quad (\text{A4})$$

which follows from the analyticity of the functions $G^{(a)}(z)$ and $C_\alpha(z)$ in the upper and lower complex half-planes. This enables to deform conveniently the integration contour into the complex plane and split it into segments containing no singularities.

Using now (A4) and the transformation rules (A3) we obtain

$$I^{(0)}(z) \rightarrow -I^{(U)}(-z), \quad I^{(U)}(z) \rightarrow -I^{(0)}(-z). \quad (\text{A5})$$

When we insert (A3), (A5) into the r.h.s. of (29a) we obtain

$$G(z) \rightarrow -G(-z) \quad (\text{A6})$$

for both sides of (29a) and hence the equations of motion obey the electron-hole symmetry.

- [1] V. Janiš and D. Vollhardt, Z. Phys. B **91**, 317 (1993)
- [2] J. Hubbard, Proc. R. Soc. London, Ser. A **281**, 401 (1964)
- [3] T. Moriya, Spin Fluctuations in Itinerant Electron Magnetism, (Springer, Berlin 1985)
- [4] G. Czycholl, Phys. Rep. **143**, 731 (1986)
- [5] G. Baym, Phys. Rev. **127**, 1391 (1962)
- [6] V. Janiš and D. Vollhardt, Int. J. Mod. Phys. B **6**, 731 (1992)
- [7] J. Hubbard, Proc. R. Soc. London, Ser. A **296**, 82 (1966)
- [8] W. Metzner, Phys. Rev. B **43**, 8549 (1991)
- [9] M. Wortis, in *Phase Transitions and Critical Phenomena*, C. Domb and M. S. Green, eds. (Academic Press, London, 1974)
- [10] A. Georges and G. Kotliar, Phys. Rev. B **45**, 6479 (1992)
- [11] M. Levine and H. Suhl, Phys. Rev. **171**, 567 (1968)
- [12] D. R. Hamann, Phys. Rev. **186**, 549 (1969)
- [13] M. C. Gutzwiller, Phys. Rev. A **134**, 923 (1964)
- [14] V. Janiš, J. Mašek, and D. Vollhardt, Z. Phys. B **91**, 325 (1993)
- [15] For a review on the physics in $d = \infty$ see D. Vollhardt, in *Correlated Electron Systems*, V. J. Emery, ed. (World Scientific, Singapore, 1993), p. 57
- [16] An approximation is called Φ -derivable if the free-energy functional can be written in closed form, see ref. [9].
- [17] G. Horwitz and H. Callen, Phys. Rev. **124**, 1757 (1961)
- [18] C. Bloch and J. S. Langer, J. Math. Phys. **6**, 554 (1965)
- [19] B. Menge and E. Müller-Hartmann, Z. Phys. B **82**, 237 (1991)
- [20] X. Y. Zhang, M. J. Rozenberg, and G. Kotliar, Phys. Rev. Lett. **70**, 1666 (1993)
- [21] A. Georges and W. Krauth, Phys. Rev. B **48**, 7167 (1993)
- [22] D. M. Edwards and J. A. Hertz, Physica B **163**, 527 (1991)
- [23] S. Wernmbter and G. Czycholl, J. Phys. C: Condensed Matter **6**, 5439 (1994)
- [24] V. Janiš and D. Vollhardt, Phys. Rev. B **46**, 15712 (1992)
- [25] To maintain the Herglotz properties during the iteration process, it is necessary that $C_\alpha(0)$ never changes its sign. The pole, if it exists, cannot move from the real axis. Although it was shown earlier in the context of the Kondo effect that full self-consistency may eventually suppress the existence of the pole in the converged solution (H. Suhl, Phys. Rev. Lett. **19**, 442 (1967)), the current iterations must be forced to keep the correct sign of the susceptibility $C_\alpha(0)$.
- [26] P.W. Anderson and G. Yuval, Phys. Rev. Lett. **23**, 89 (1969)

Figure Captions

- Fig.1** DOS at weak coupling calculated from the LCE with U^2 -corrections to the Hartree-Fock MFT at $U = 1.4$ (broken line) and $U = 1.7$ (solid line). We used the semi-elliptic DOS with the bandwidth $2D = 4$.
- Fig.2** DOS at $U = 1.9$ in the same theory as in Fig.1. For larger U 's the iterations do not converge any longer.
- Fig.3** DOS calculated with the iterated perturbation theory (IPT) within the domain of convergence of iterations, $U = 1.7, 2.7, 4.7$ depicted as dotted, broken and solid lines, respectively.
- Fig.4a** Real part of the propagator $G^{(0)}$ within IPT for $U = 1.7, 3.7, 4.7$ as in Fig.3.
- Fig.4b** Imaginary part of $G^{(0)}$ within IPT for the same values of U as in Fig.4a.
- Fig.5** The location ω_{min} of the minima in $\text{Re}G^{(0)}(\omega)$ (broken line) and $\text{Im}G^{(0)}(\omega)$ (solid line).
- Fig.6** DOS for the IPT extended of the ring diagrams at $U = 1.87$.
- Fig.7** Simplest diagrams contributing to the expansion of the exponential in (20). The hatched bubbles represent the function C , the wavy lines derivatives w.r.t. generating sources.
- Fig.8** DOS for the fully self-consistent approximation with the ring diagrams around the Hartree-Fock MFT at $U = 1.5$ (broken line) and $U = 3.5$ (solid line).
- Fig.9** DOS for the fully self-consistent approximation with the ring diagrams around the strong-coupling MFT at $U = 1.5$ (broken line), $U = 3.5$ (dotted line), and $U = 5$ (solid line).
- Fig.10a** Contribution to the imaginary part of the self-energy $\Delta\Sigma$ due to the ring diagrams at $U = 3.5$ for the strong-coupling (broken line) and the Hartree-Fock (solid line) MFT.
- Fig.10b** Contribution to the imaginary part of the self-energy $\Sigma - \Delta\Sigma$ due the Hubbard-III term in the static strong-coupling MFT (broken line) and the dynamic MFT with ring diagrams (solid line) at $U = 3.5$.

Fig.1

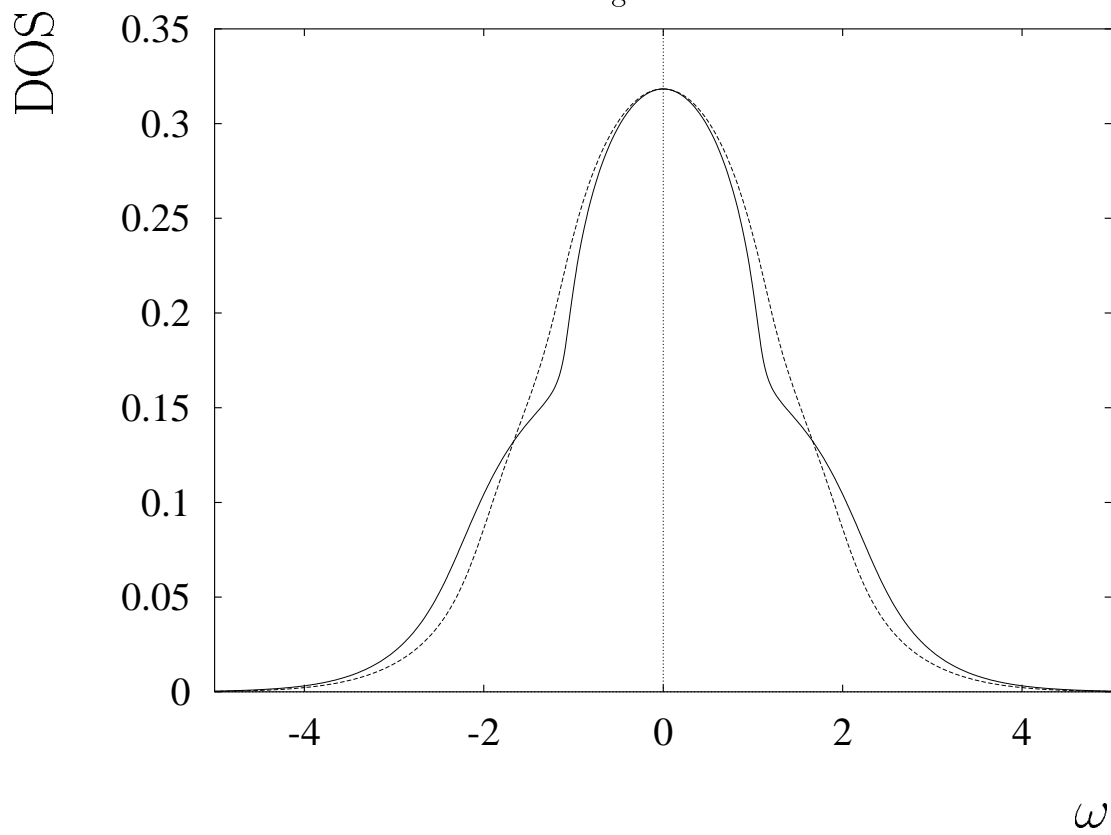


Fig.2

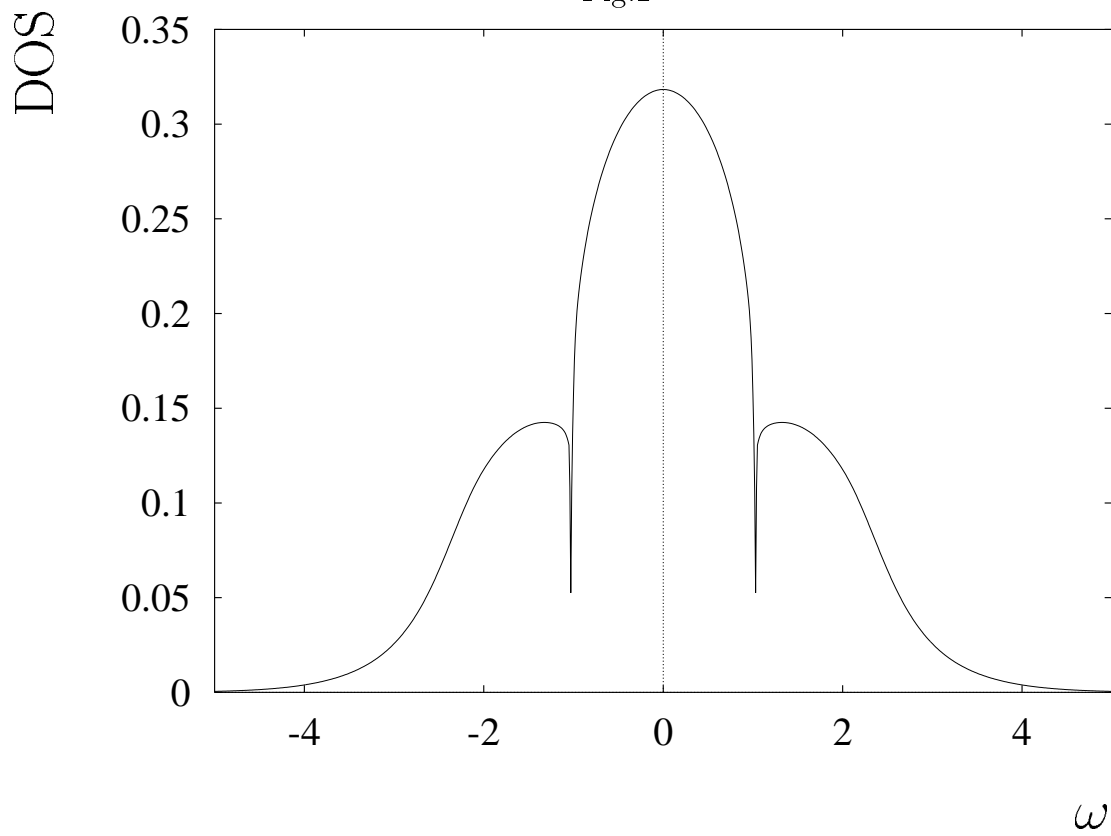


Fig.3

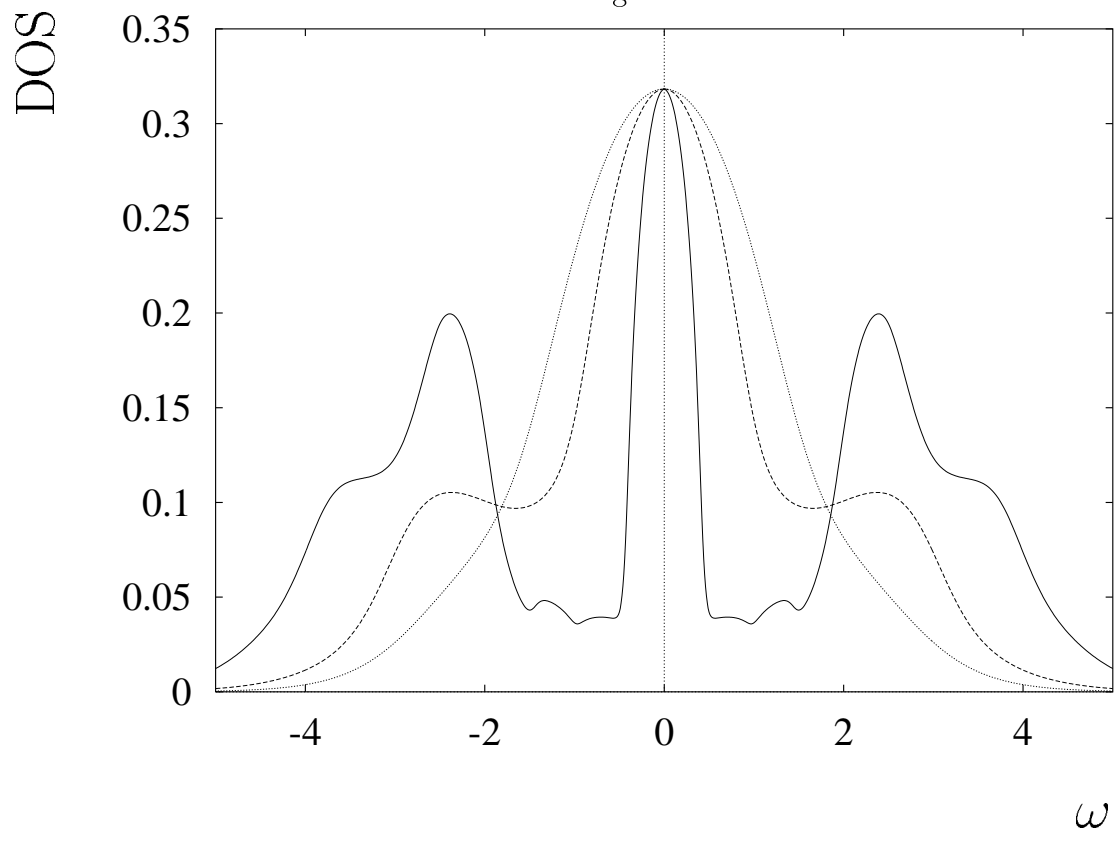


Fig.4a

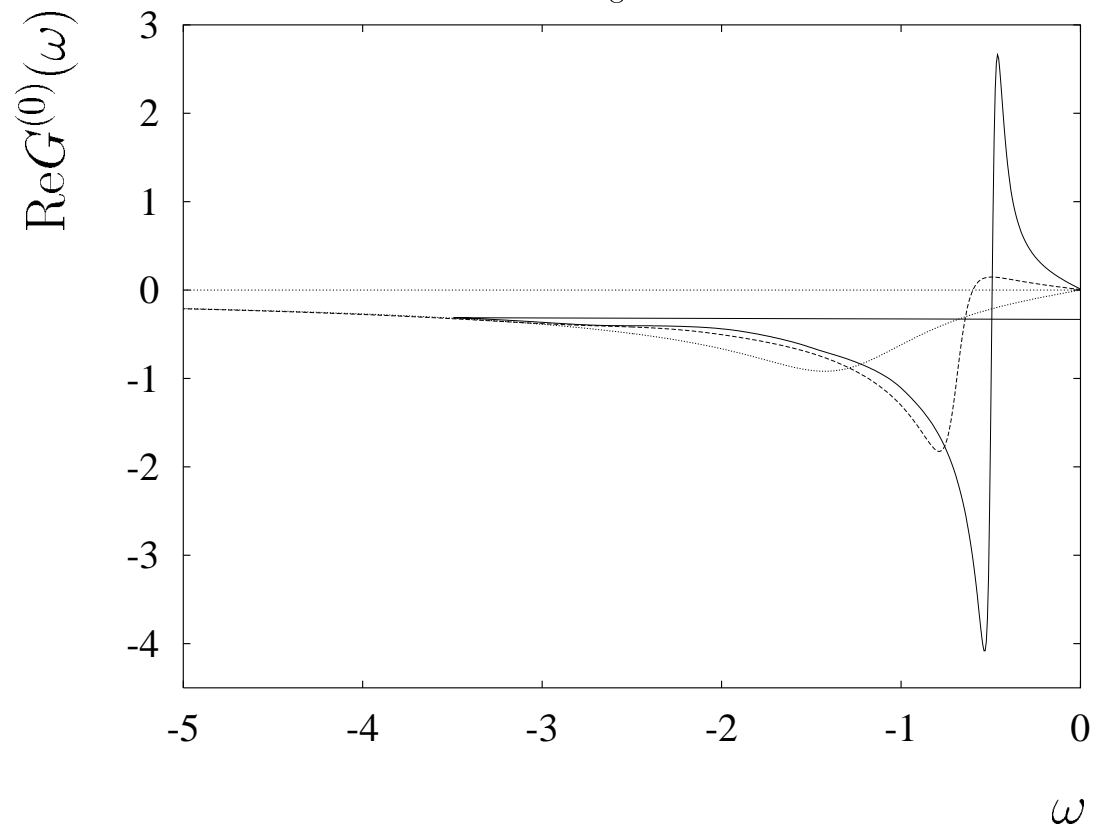


Fig.4b

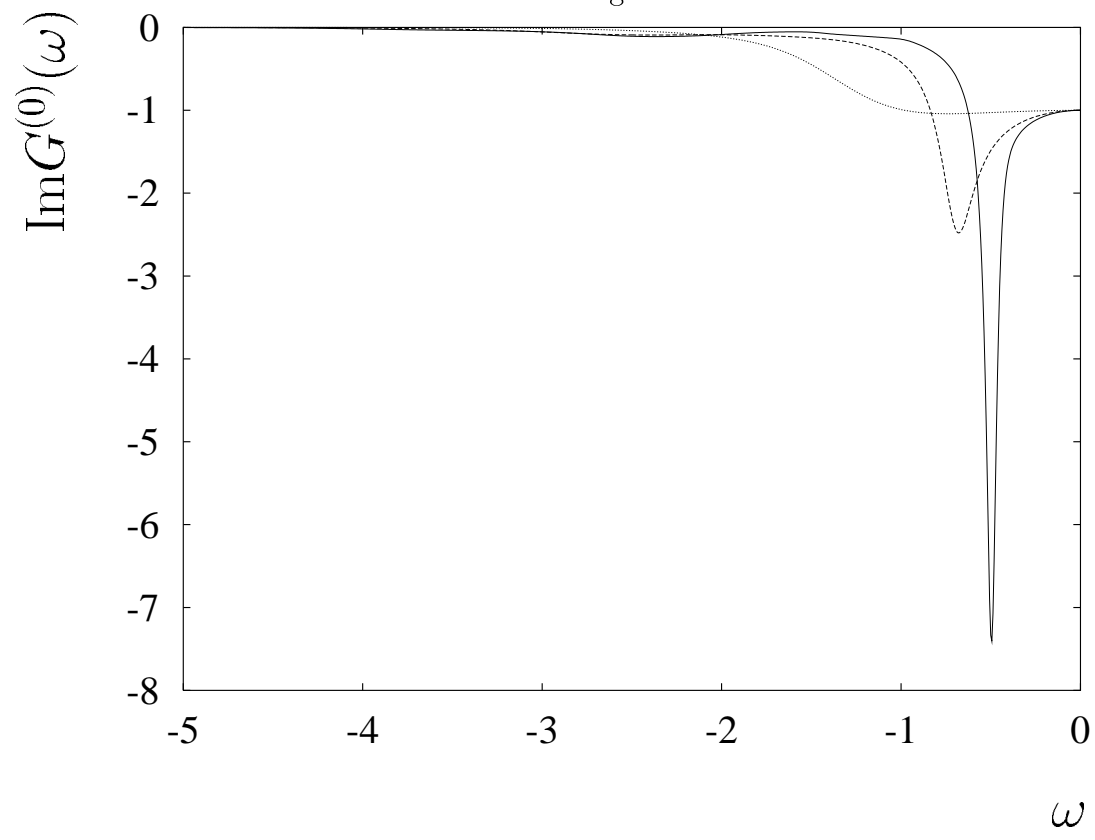


Fig.5

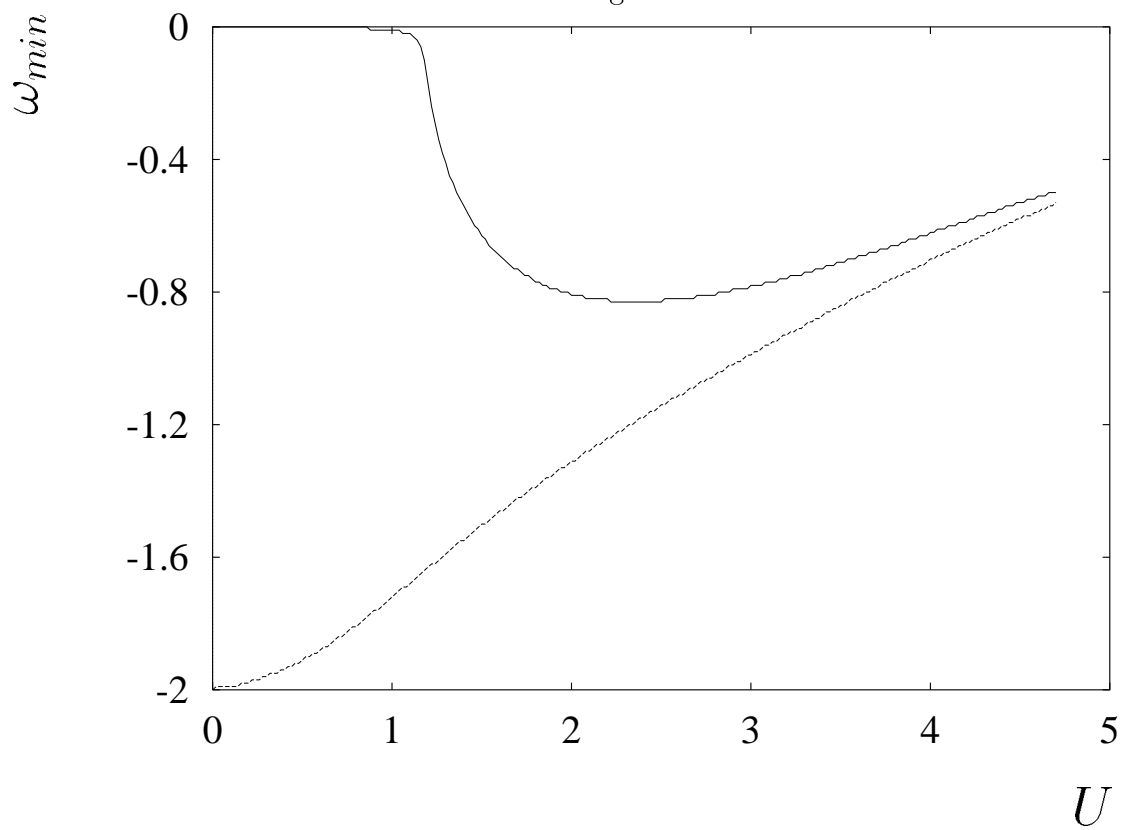


Fig.6

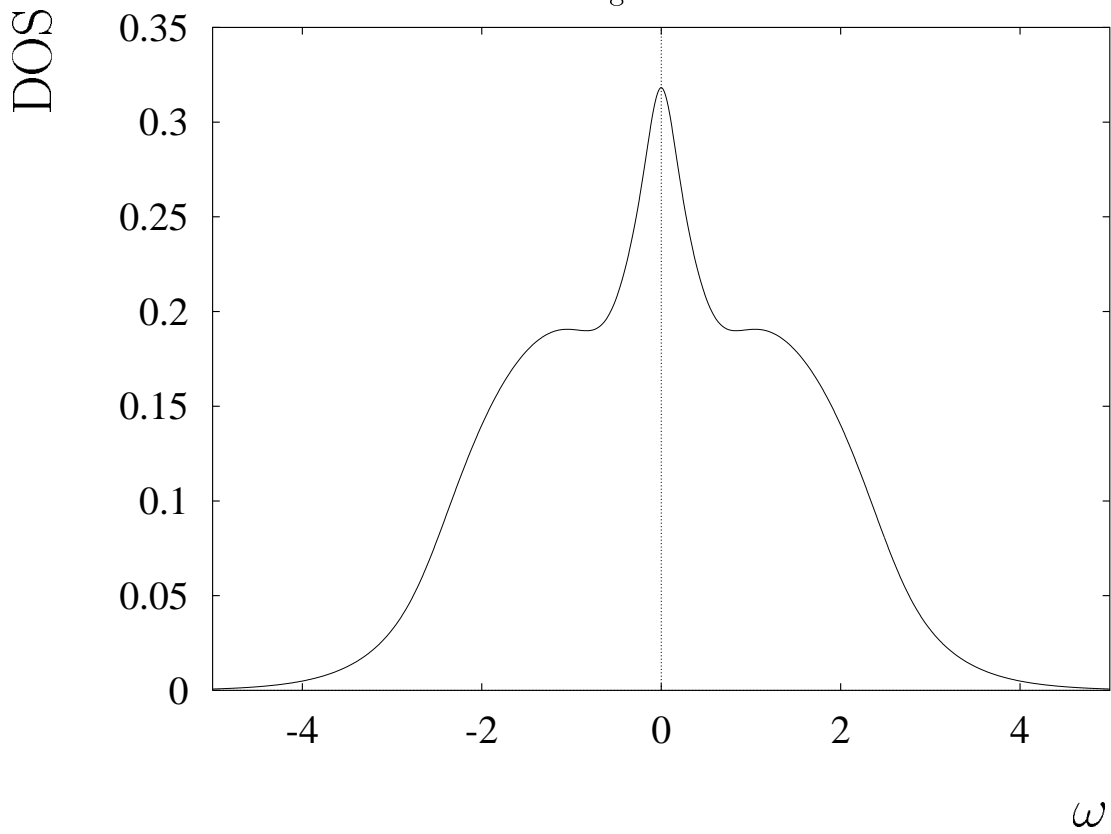


Fig.7

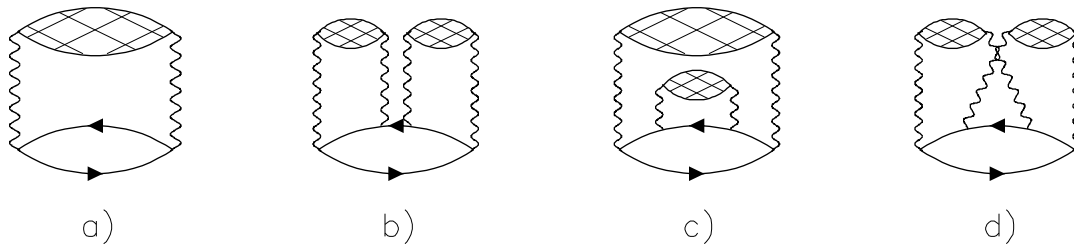


Fig.8

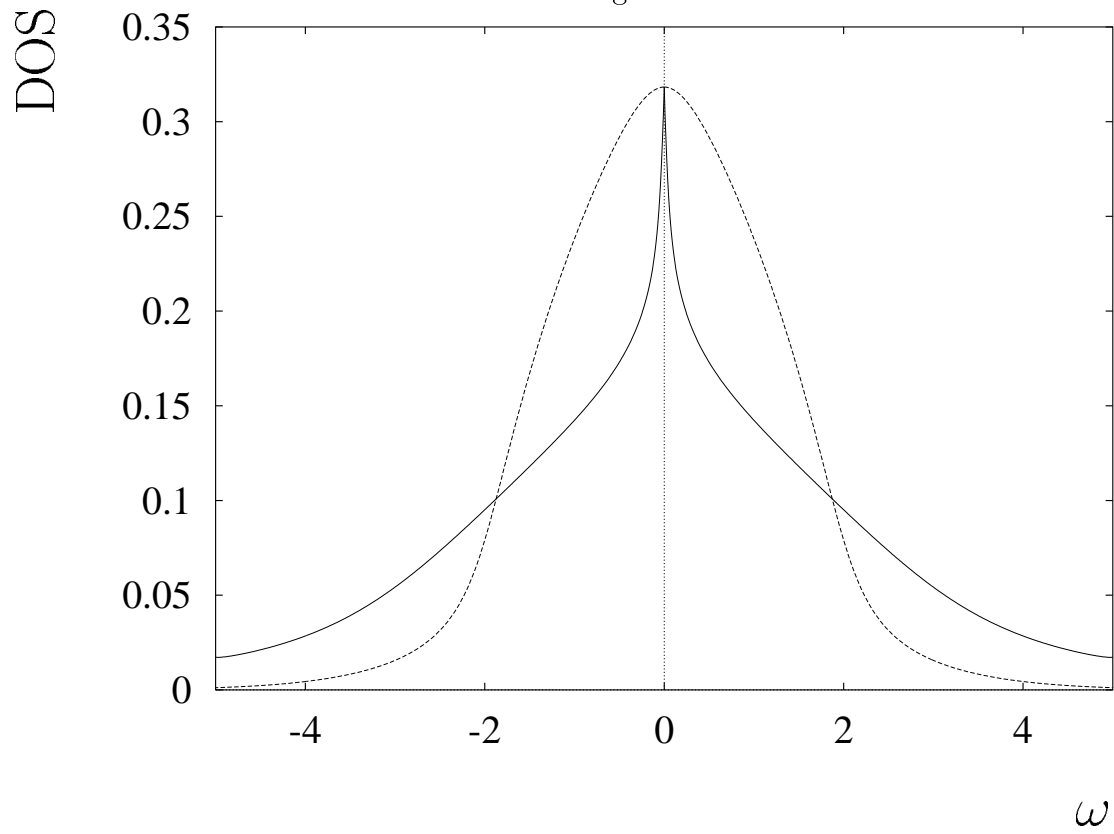


Fig.9

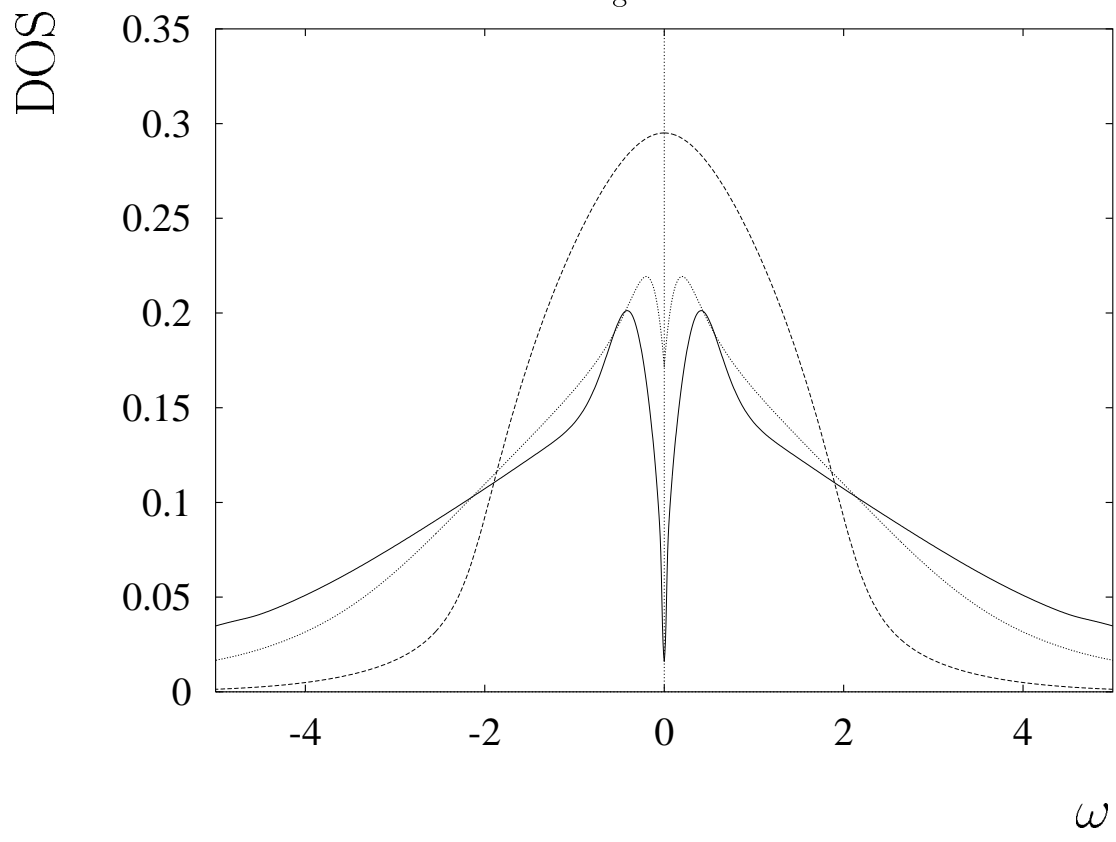


Fig.10a

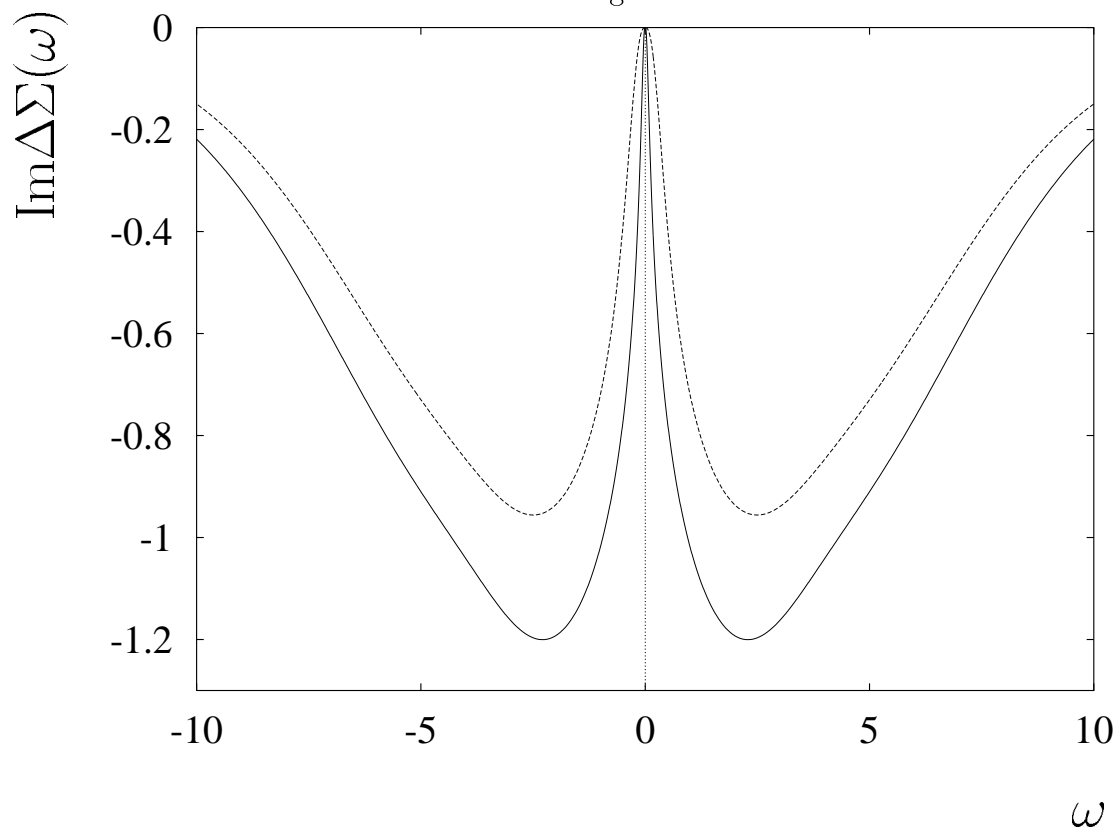


Fig.10b

